I THERMOCHEMISTRY AND REACTION KINETICS OF DISOLVATED PROTONS BY ION CYCLOTRON RESONANCE SPECTROSCOPY

II THERMOCHEMICAL STUDIES OF SMALL FLUOROCARBONS BY PHOTOIONIZATION MASS SPECTROMETRY

Thesis by

D. Wayne Berman

In Partial Fulfillment of the Requirements

For the Degree of

Doctor of Philosophy

California Institute of Technology

Pasadena, California

1981

(Submitted December 1 , 1980)

To Andi

ACKNOWLEDGEMENTS

I would like to thank Jack Beauchamp for sharing the secrets of good story-telling. His patience and advice concerning matters both in and out of field were never lacking. Other members of the Beauchamp group, past and present, must be acknowledged for sharing the good times and the not so good times.

Projects employing the photoionization mass spectrometer presented an opportunity to interact with a number of JPL residents who provided useful discussions in addition to making lunch-time entertaining. I would especially like to acknowledge Vince Anicich for his part in maintaining a stimulating and lively atmosphere in room 163.

Those who helped to freshen the spice of life include Carol Oken, Joe Griffith and the never-quite-gang-of-four I had the pleasure to share a house with over the years. Dave Edmundson and the rest of the undergrounders helped to keep the fat off. I would especially like to thank a close friend, Jenna Zinck, for helping me to maintain some semblence of sanity during the writing of this work. My family, Steve Goldenberg and the rest of the Eastern contingent have been continual sources of stability in the face of change.

Finally, I would like to thank Henriette Wymar for typing the majority of this thesis on such short notice, and Emily Olsen for taking care of the finishing touches.

ABSTRACT

The disolvated proton, $H(OH_2)_2^+$ is employed as a chemical reagent in low pressure ($<10^{-5}$ torr) investigations by ion cyclotron resonance spectroscopy. Since termolecular reactions are absent at low pressure, disolvated protons are not generally observed. However, $H(OH_2)_2^+$ is produced in a sequence of bimolecular reactions in mixtures containing H_2O and one of a small number of organohalide precursors. Then a series of hydrated Lewis bases is produced by H_3O^+ transfer from $H(OH_2)_2^+$. In Chapter II, the relative stability of hydrated bases containing heteroatoms of both first and second row elements is determined from the preferred direction of H_3O^+ transfer between $BH(OH_2)^+$ complexes. S and P containing bases are shown to bind H_3O^+ more weakly than O and N bases with comparable proton affinities. A simple model of hydrogen bonding is proposed to account for these observations.

H^+ transfer from $H(OH_2)_2^+$ to several Lewis bases also occurs at low pressure. In Chapter III the relative importance of H_3O^+ transfer and H^+ transfer from $H(OH_2)_2^+$ to a series of bases is observed to be a function of base strength. Beginning with CH_3COOH, the weakest base for which H^+ transfer is observed, the importance of H^+ transfer increases with increasing proton affinity of the acceptor base. The nature of neutral products formed from $H(OH_2)_2^+$ by loss of H^+ is also considered.

Chapters IV and V deal with thermochemistry of small fluorocarbons determined by photoionization mass spectrometry. The enthalpy of formation of CF_2 is considered in Chapter IV. Photoionization of perfluoropropylene, perfluorocyclopropane, and trifluoromethyl benzene yield onsets for ions formed by loss of a CF_2 neutral fragment. Earlier

determinations of ΔH_{f298}° (CF_2) are reinterpreted using updated thermochemical values and compared with results of this study. The heat of formation of neutral perfluorocyclopropane is also derived. Finally, the energetics of interconversion of perfluoropropylene and perfluorocyclopropane are considered for both the neutrals and their molecular ions.

In Chapter V the heats of formation of CF_3^+ and CF_3I^+ are derived from photoionization of CF_3I. These are considered with respect to ion-molecule reactions observed in CF_3I monitored by the techniques of ion cyclotron resonance spectroscopy. Results obtained in previous experiments are also compared.

TABLE OF CONTENTS

CHAPTER I

INTRODUCTION

INTRODUCTION

One of the advantages of probing phenomena in the gas phase is that observed behavior depends only on the nature of the isolated species present. Intrinsic properties are not masked by solvation. For example, relative acidities and basicities for a large number of gas phase species have been determined by ion cyclotron resonance spectroscopy,[1,2,3] high pressure mass spectrometry[1,4,5] and flowing afterglow techniques.[1,6] When trends observed in the two phases can be compared, such gas phase studies often facilitate an understanding of the more complicated processes that occur in solution. Differences are accounted for by the effects of solvation.[7] To relate gas phase and solution chemistry systematically, however, it is necessary to quantify direct interactions between solvent and solute molecules.

A number of investigators have reported association energies for ions with a small number of solvent molecules.[4-6,8,9] These studies consider proton bound complexes which are usually generated by direct association, equation 1, at pressures above 10^{-3} torr. Equation 1

$$B + HB^{+}_{(n-1)} \rightarrow [HB^{+}_{n}]^{*} \xrightarrow{[M]} HB^{+}_{n} \qquad (1)$$

represents a termolecular process where intermediates produced during encounters between the reactants must be stabilized by collision with a third body M. Such processes are unimportant at reduced particle densities. However, a series of fortuitous discoveries over the past several years have presented the possibility of studying proton bound dimers at lower pressures ($<10^{-5}$ torr).

During trapped ion ICR studies[10] of a series of exchange reactions among small onium ions, equation 2, production of $H(OH_2)_2^+$ was observed in a mixture of CH_3CHCl_2 and H_2O. Further experimentation revealed

$$CH_3CHX^+ + YH \rightarrow CH_3CHY^+ + XH \quad (X, Y = Cl, Br, OH, SH, NH_2, PH_2) \quad (2)$$

that $H(OH_2)_2^+$ is produced via a sequence of bimolecular reactions in this mixture and that the same process occurs in mixtures of H_2O and CH_3CHBr_2 as well.[11] Meanwhile, measuring the proton affinities of species less basic than H_2O, Clair and McMahan[12] discovered $H(OH_2)_2^+$ is similarly produced by a bimolecular reaction sequence in mixtures of $(CF_2H)_2O$ and H_2O. It is thus possible to study the chemistry of $H(OH_2)_2^+$ using low pressure techniques such as ion cyclotron resonance spectroscopy.

Chapters II and III of this thesis represent two applications of techniques developed in the earlier ICR investigations[11] of $H(OH_2)_2^+$ to problems of interest. Since periodic trends in ion-solvent interactions are not well characterized, stabilities were determined for a series of hydrated bases containing heteroatoms of both first and second row elements. As described in Chapter II, hydrated bases are generated by H_3O^+ transfer from $H(OH_2)_2^+$. Then trapped ion ICR studies of the preferred direction of H_3O^+ transfer between base pairs permit the assignment of relative stabilities for each species. Competition between H^+ transfer and H_3O^+ transfer from $H(OH_2)_2^+$ to a series of n-donor bases, eq. 3 and 4, is the subject of Chapter III. Such a study would be complicated at higher pressures by direct association of the protonated base, BH^+, with H_2O, eq. 5. Trapped ion ICR techniques are therefore

$$B + H(OH_2)_2^+ \longrightarrow BH(OH_2)^+ + H_2O \quad (3)$$

$$B + H(OH_2)_2^+ \longrightarrow BH^+ + (H_2O)_2 \quad (4)$$

$$BH^+ + H_2O \rightarrow BH(OH_2)^+ \quad (5)$$

particularly suited to this application.

In another set of studies, chapters IV and V represent further examples of the value of photoionization mass spectrometry in elucidating thermochemistry for species of interest in a variety of investigations. Photoionization mass spectrometry is a proven technique for untangling the thermochemistry of ions, and neutral fragments.[13] When thermal energy contributions can be accounted for, PIMS measurements and related thermodynamic quantities derived from these studies are typically precise within 20 meV.[14,15] Thus PIMS studies related to many aspects of research in this laboratory have been useful. For example, the enthalpies of formation of halonium ion structural isomers $C_2H_4X^+$ (X = Cl, Br) were determined from appearance potential measurements of such ions from 1,1- and 1,2-dihaloethane precursors.[10] In another study involving rare gas molecular ions,[16] XeF^+ formation was shown to result exclusively from reaction of the excited $^2P_{\frac{1}{2}}$ state of Xe^+, eq. 6. More recently, relative energies of metal-hydrogen and

$$(Xe^+)^* + NF_3 \rightarrow XeF^+ + NF_2 \quad (6)$$

metal carbon bonds were determined for a series of complexes $(CO)_5MnR$ (R = H, CH_3, CH_2F, CHF_2, and CF_3). Relative metal-carbene bond energies for the ions $(CO)_5Mn^+$-CXY (X, Y = H, F) were also obtained.[17] The present studies deal with thermochemistry of fluoro-

carbons. In Chapter IV, the enthalpy of formation of CF_2 is determined from threshold energies of ions produced by CF_2 loss from a series of fluorocarbons including perfluoropropylene and perfluorocyclopropane. Questions concerning the energetics of interconversion for both neutral and ion C_3F_6 isomers are also addressed. In Chapter V the heat of formation of CF_3^+ is derived from the threshold energy for process 7. Results are discussed in light of other measurements and related thermochemistry of a series of small fluorocarbons.

$$CF_3I + h\nu \rightarrow CF_3^+ + I \qquad (7)$$

References

(1) For a general overview see: Bowers, M. T. "Gas Phase Ion Chemistry", Vol. 2; Academic Press, New York, 1979.

(2) Wolf, J. F ; Staley, R. H.; Koppel, I.; Taagepera, M.; McIver, R. T.; Beauchamp, J. L.; and Taft, R. W. J. Am. Chem. Soc. 1977, 99, 5417.

(3) Bartmess, J. E.; Scott, J. A.; and McIver, R. T. J. Am. Chem. Soc., 1979, 101, 6046.

(4) Yamdagni, R.; and Kebarle, P. J. Am. Chem. Soc. 1976, 98, 1320.

(5) Kebarle, P.; Ann. Rev. Phys. Chem. 1977, 28, 445.

(6) Fehsenfeld, F. C.; and Ferguson, E. E.; J. Chem. Phys. 1973, 59, 6272.

(7) For example: Arnett, E. M.; Jones III, F. M.; Taagepera, M.; Henderson, W. G.; Beauchamp, J. L.; Holtz, D.; and Taft, R. W. J. Am. Chem. Soc. 1972, 94, 4724.

(8) Olmstead, W. N.; Lev-On, M.; Golden, D. M.; and Brauman, J. I. J. Am. Chem. Soc. 1977, 99, 992.

(9) Meot-Ner, M.; and Field, F. H. J. Chem. Phys. 194, 61, 3742.

(10) Berman, D. W.; Anicich, V.; and Beauchamp, J. L. J. Am. Chem. Soc. 1979, 101, 1239.

(11) Berman, D. W.; and Beauchamp, J. L. J. Phys. Chem. 1980, 84, 2233.

(12) Clair, R. L.; and McMahan, T. B. Can. J. Chem. 1980, 58, 863.

(13) See for example: Chupka, W. A. "Ion Molecule Reactions", Vol. 1, J. L. Franklin, ed., 1972, Plenum Press, New York.

References (continued)

(14) Chupka, W. A. J. Chem. Phys. 1959, 30, 191.

(15) Chupka, W. A. J. Chem. Phys. 1970, 54, 1936.

(16) Armentrout, P. B.; Berman, D. W.; and Beauchamp, J. L. Chem. Phys. Lett. 1978, 53, 255.

(17) Stevens, A. E.; Berman, D. W.; and Beauchamp, J. L. J. Am. Chem. Soc. to be submitted.

CHAPTER II

CHEMISTRY OF DISOLVATED PROTONS. PERIODIC TRENDS IN THE RELATIVE STABILITY OF HYDRATED BASES DETERMINED FROM THE PREFERRED DIRECTION OF H_3O^+ TRANSFER BY ION CYCLOTRON RESONANCE SPECTROSCOPY

Chemistry of Disolvated Protons. Periodic Trends in the Relative Stability of Hydrated Bases Determined from the Preferred Direction of H_3O^+ Transfer by Ion Cyclotron Resonance Spectroscopy

D. W. Berman and J. L. Beauchamp

Contribution No. from the Arthur Amos Noyes Laboratory of Chemical Physics, California Institute of Technology, Pasadena, California 91125. (Received)

Abstract

The relative stability of hydrated bases containing heteroatoms of both first and second row elements is determined from the preferred direction of H_3O^+ transfer between $BH(OH_2)^+$ complexes. S and P containing bases systematically bind H_3O^+ more weakly than O and N bases with comparable proton affinities. A simple model of hydrogen bonding is proposed to account for these observations. $BH(OH_2)^+$ complexes are produced by H_3O^+ transfer from $H(OH_2)_2^+$. A bimolecular reaction sequence yielding $H(OH_2)_2^+$ in a mixture of CH_3CHF_2 and H_2O is introduced and compared with $H(OH_2)_2^+$ production in similar mixtures.

I. Introduction

Several topics of current chemical interest can be addressed by studies of proton bond clusters. In addition to their importance as participants in the chemistry of the upper atmosphere,[1-3] proton bound complexes represent probable reaction intermediates for a number of ion-molecule processes[4-9] including proton transfer[10-13] and nucleophilic displacement.[14-17] Hydrogen bonding in these species involves delocalization of electrons over several nuclear centers so that proton bound clusters provide examples of non-classically bonded structures.[18-24] Further, viewing such complexes as protonated bases associated with a small number of solvent molecules underscores their importance in understanding the relationship between gas phase and solution chemistry.[25-33] A number of these species have also been used as reagents in chemical ionization experiments.[34-37]

Normally, proton bound dimers and larger clusters are generated at pressures above 10^{-3} torr by direct association, eq. 1.[5-8,19,30]

$$B_1H^+ + B_2 \rightarrow [B_1HB_2^+]^* \xrightarrow{[m]} B_1HB_2^+ \qquad (1)$$

In eq. 1, encounters between a protonated base BH^+ and a Lewis base B_2 form an excited intermediate $[B_1HB_2^+]^*$ which must be stabilized by collision with a third body M to be observed. Once generated, the relative stability of these dimers is obtained either from the temperature dependence of equilibrium between reactants and products of the association reactions producing a specific cluster, eq. 1, or from the preferred direction of exchange between complexes containing a common

reference base B_0, eq. 2. It should be no surprise that the most

$$B_1HB_0^+ + B_2 \rightleftharpoons B_2HB_0^+ + B_1 \qquad (2)$$

abundant solvent, water, has been the reference base most commonly employed in these studies.

Monitoring exchange reactions is expedited when contributions from condensation reactions are curtailed as in low pressure ICR trapped ion experiments ($< 10^{-5}$ torr). A large number of relative acidities,[38] eq. 3, and basicities,[39] eq. 4, have already been deter-

$$A_1H + A_2^- \rightleftharpoons A_2H + A_1^- \qquad (3)$$

$$B_1H^+ + B_2 \rightleftharpoons B_2H^+ + B_1 . \qquad (4)$$

mined by this technique. The possibility of extending these ICR studies to include hydrated proton transfer, eq. 5, has been facilitated

$$B_1H(OH_2)^+ + B_2 \rightarrow B_2H(OH_2)^+ + B_1 \qquad (5)$$

by discoveries of specific organohalide molecules that react with H_2O via a sequence of bimolecular reactions ultimately yielding $H(OH_2)_2^+$. Then, by further sequential substitution, eqs. 6 and 7, a greater

$$H(OH_2)_2^+ + B \rightarrow BH(OH_2)^+ + H_2O \qquad (6)$$

$$B_1H(OH_2)^+ + B_2 \rightarrow B_1HB_2^+ + H_2O \qquad (7)$$

number of generalized solvated proton transfers, eq. 2, can also be studied.

The mechanism of $H(OH_2)_2^+$ production in a mixture of CH_3CHF_2 and

H_2O is presented and compared with results previously reported for mixtures containing CH_3CHCl_2,[33] CH_3CHBr_2,[33] and $(CF_2H)_2O$.[40] In addition, results of a study of solvated proton transfer, eq. 5, between a number of bases containing heteroatoms of both first and second row elements are reported. Periodic trends inferred from such H_3O^+ transfer reactions are correlated with trends observed for other properties of bases including proton affinities[39] and lithium ion affinities.[41]

II. Experimental

Ion cyclotron resonance instrumentation and techniques have been previously described in detail.[42-44] Experiments were carried out at ambient temperature (25° C). Neutral pressures ranged between 1.0×10^{-8} - 1.0×10^{-5} torr. Pressures were measured on a Schulz-Phelps type ionization gauge calibrated against an MKS Baratron Model 90H1-E capacitance manometer. Pressures measured by this technique should be accurate to ± 20%. Except as noted, chemicals used in this work were obtained from commercial sources. HCN was generated from KCN and acid, and distilled under vacuum. Formaldehyde was prepared fresh before each experiment from thermal decomposition of paraformaldehyde. All samples were degassed by several freeze-pump-thaw cycles to remove noncondensable contaminants.

III. Results

Gas Phase Ion Chemistry of the Organohalide Precursors of $H(OH_2)_2^+$: 1,1-dihaloethanes and bisdifluoromethyl ether. Ions produced

by 70 eV electron impact of CH_3CHF_2 at 7×10^{-8} torr are HCF_2^+ (45%), $CH_3CF_2^+$ (25%), CH_3CHF^+ (22%), and CH_2CF^+ (8%). No molecular ion is observed. This can be contrasted with the mass spectra of CH_3CHCl_2 or CH_3CHBr_2 where small parent peaks (5%) are present, the major fragment ion is CH_3CHX^+ (80%), and small contributions from $C_2H_3^+$, X^+, XH^+, and HCX_2^+ (X = Cl, Br) make up the remainder of the spectra after 70 eV electron impact.[45] Gas phase ion chemistry of all CH_3CHX_2 (X = F, Cl, Br) species are equivalent. As illustrated by the temporal variation of ion abundance observed in CH_3CHF_2 upon ionization by 70 eV electrons presented in Figure 1, the only species remaining at long times is the fluoroethyl cation CH_3CHF^+. Other fragments all react by fluoride transfer to yield CH_3CHF^+ as confirmed by double resonance ejection techniques. Similarly, CH_3CHX^+ is the only major species remaining at long times during trapped ion experiments in CH_3CHCl_2 and CH_3CHBr_2.[45]

As previously reported,[40] the dominant ion in the bisdifluoromethyl ether $(CF_2H)_2O$ mass spectrum at an electron energy of 70 eV is CF_2H^+. This ion reacts with $(CF_2H)_2O$ by the fluoride abstraction reaction 8.[40]

$$CF_2H^+ + (CF_2H)_2O \rightarrow CF_2HOCFH^+ + CF_3H \quad . \qquad (8)$$

Mixtures of 1,1-dihaloethanes and water as sources of $H(OH_2)_2^+$. When H_2O is added to CH_3CHF_2, a sequence of reactions occurs identical to those reported in CH_3CHCl_2 and CH_3CHBr_2.[33] The temporal variation of ion abundance following a 70 eV electron pulse in a 13.5:1 mixture of H_2O and CH_3CHF_2 at a total pressure of 1.1×10^{-6} torr is

FIGURE 1. Variation of ion abundance with time following a 20 msec, 70.0 eV electron beam pulse in CH_3CHF_2 at 1.1×10^{-7} torr.

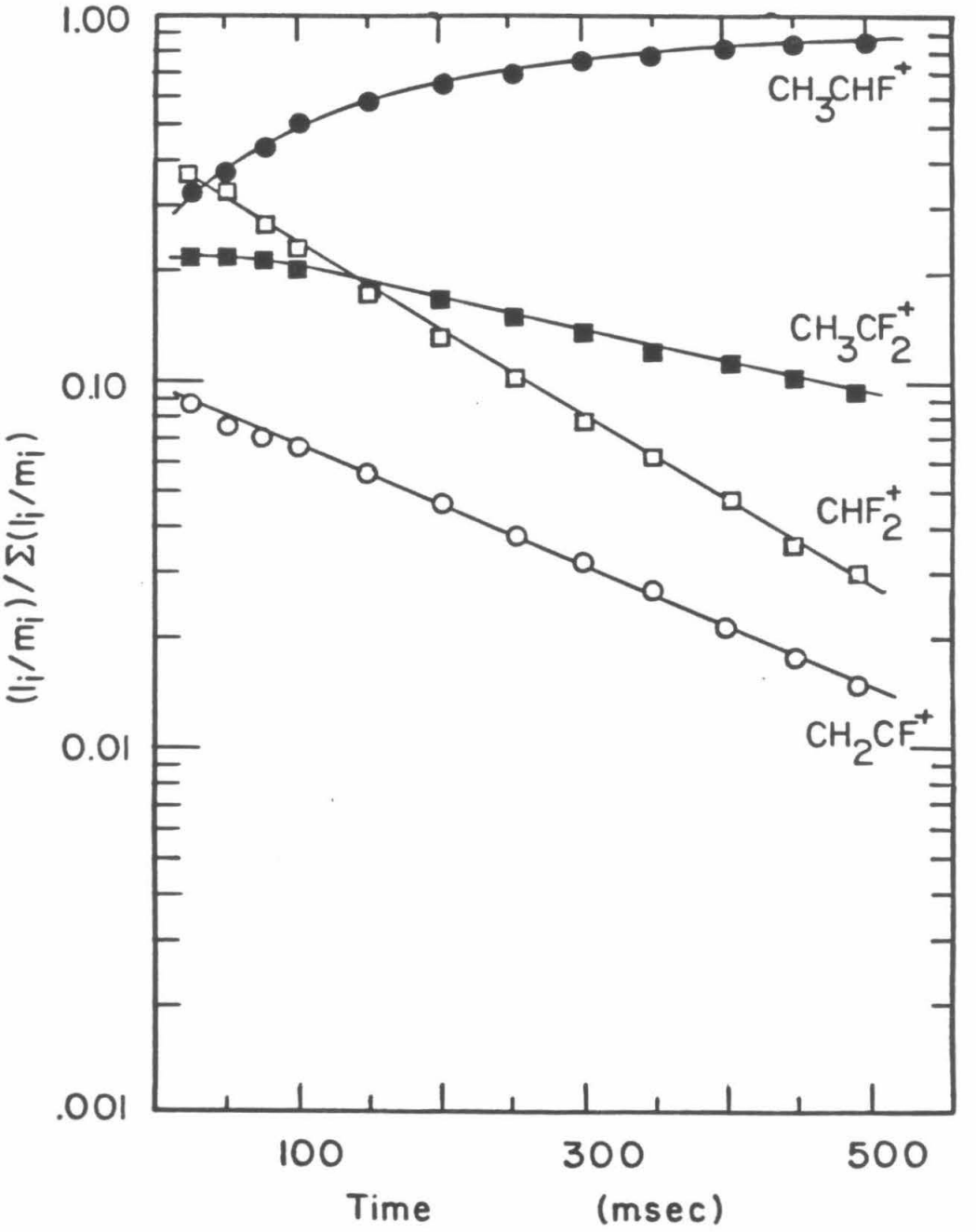
1.00
0.10
0.01
.001
$(I_i/m_i) / \Sigma(I_i/m_i)$
CH_3CHF^+
$CH_3CF_2^+$
CHF_2^+
CH_2CF^+
100
300
500
Time
(msec)

presented in Figure 2.[46] Briefly, H_3O^+ reacts with CH_3CHF_2 forming a bifunctional intermediate $CH_3CHF(OH_2)^+$ by loss of HF, eq. 9. In 53% of these encounters, the bifunctional intermediate retains sufficient excess internal energy to eliminate a second molecule of HF, eq. 10.

$$H_3O^+ + CH_3CHF_2 \begin{cases} \xrightarrow{47\%} CH_3CHF(OH_2)^+ + HF & (9) \\ \xrightarrow{53\%} CH_3CHOH^+ + 2HF & (10) \end{cases}$$

The product of reaction 9 reacts further with H_2O to yield the disolvated proton, eq. 11. $H(OH_2)_2^+$ (37%) produced in reaction 11, CH_3CHOH^+ (41%)

$$CH_3CHF(OH_2)^+ + H_2O \rightarrow H(OH_2)_2^+ + CH_2CHF \qquad (11)$$

from eq. 8, and CH_3CHF^+ (12%) which is unreactive in this mixture[47] are the major species at long times. The relative importance of processes 9 and 10 depends somewhat on pressure. The maximum yield of $H(OH_2)_2^+$, comprising 56% of the total ion concentration at long times, obtained in a 26:1 mixture of H_2O and CH_3CHF_2 at a total pressure of 2.0×10^{-6} torr. Under these conditions, 60% of the encounters between H_3O^+ and CH_3CHF_2 proceed via reaction 9.

<u>$H(OH_2)_2^+$ derived in a mixture of $(CF_2H)_2O$ and H_2O.</u> Figure 3 depicts the temporal variation of ion abundance in a 3.5:1 mixture of H_2O and $(CF_2H)_2O$ at a total pressure of 8.9×10^{-7} torr. Chemistry observed in this mixture concurs with results reported earlier[40] except for the observation of two previously unreported minor ions, $HFH(OH_2)^+$ and $HCFOH^+$, comprising less than 7% of the total ion concentration at all times. As in the earlier study,[40] the only ion persisting at long

FIGURE 2. Variation of ion abundance with time following a 20 msec, 70.0 eV electron beam pulse in a 1:13.5 mixture of CH_3CHF_2 and H_2O at a total pressure of 1.1×10^{-6} torr.

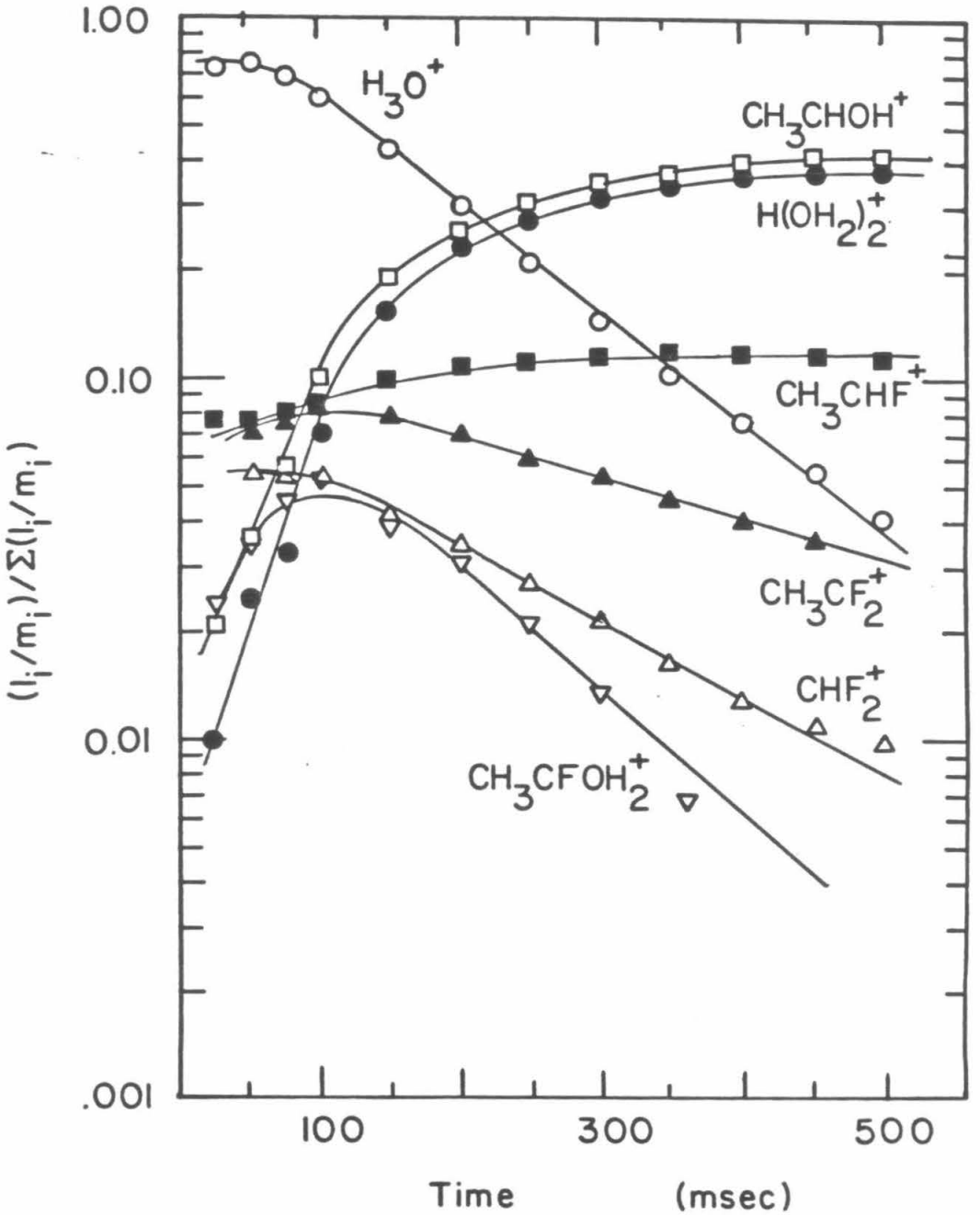
1.00
0.10
0.01
.001
100
300
500
Time (msec)
$(I_i/m_i)/\Sigma(I_i/m_i)$
H_3O^+
CH_3CHOH^+
$H(OH_2)_2^+$
CH_3CHF^+
$CH_3CF_2^+$
CHF_2^+
$CH_3CFOH_2^+$

FIGURE 3. Variation of ion abundance with time following a 20 msec, 70.0 eV electron beam pulse in a 1:3.5 mixture of $(CF_2H)_2O$ and H_2O at a total pressure of 8.9×10^{-7} torr.

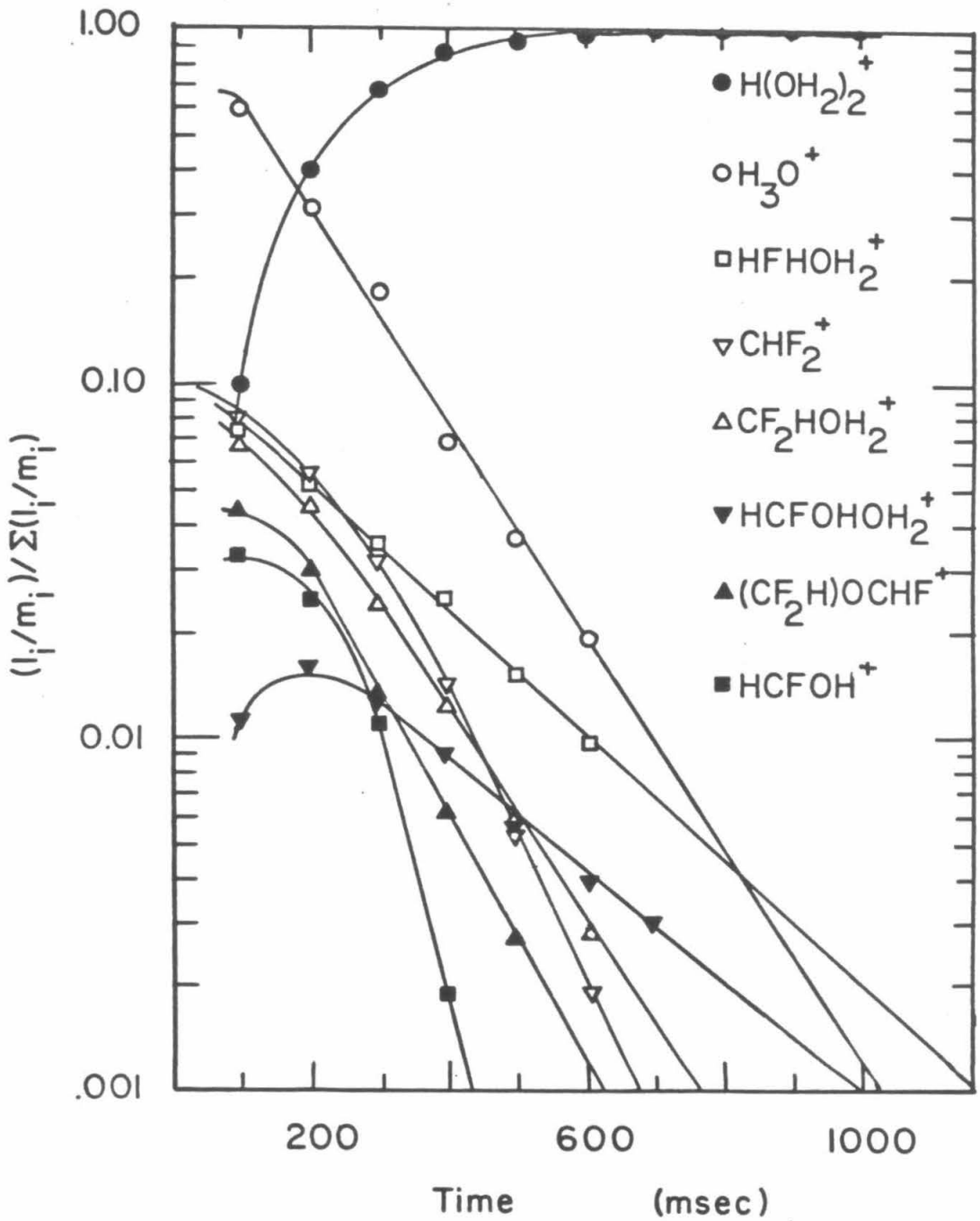
1.00
0.10
0.01
.001
200
600
1000
Time (msec)
$(I_i/m_i)/\Sigma(I_i/m_i)$
$H(OH_2)_2^+$
H_3O^+
$HFHOH_2^+$
CHF_2^+
$CF_2HOH_2^+$
$HCFOHOH_2^+$
$(CF_2H)OCHF^+$
$HCFOH^+$

times is $H(OH_2)_2^+$, a product of two independent reaction sequences. The first is initiated when CF_2H^+ reacts to yield CF_2HOCHF^+ as in $(CF_2H)_2O$ alone, reaction 8. Then, CF_2HOCFH^+ reacts sequentially with two molecules of H_2O, eqs. 12 and 13, ultimately yielding $H(OH_2)_2^+$.

$$CF_2HOCHF^+ + H_2O \rightarrow CF_2HOH_2^+ + HCFO \quad (12)$$

$$CF_2HOH_2^+ + H_2O \rightarrow H(OH_2)_2^+ + CF_2 \quad (13)$$

In the second sequence, an encounter between H_3O^+ and $(CF_2H)_2O$ produces the proton bound complex of fluoroformate and water $HCFOH(OH_2)^+$, eq. 14, which transfers a hydrated proton to a second

$$H_3O^+ + (CF_2H)_2O \rightarrow HCFOH(OH_2)^+ + CF_3H \quad (14)$$

H_2O molecules yielding $H(OH_2)_2^+$, eq. 15. Double resonance experiments

$$HCFOH(OH_2)^+ + H_2O \rightarrow H(OH_2)_2^+ + HCFO \quad (15)$$

suggest that in a fraction of encounters producing $HCFOH(OH_2)^+$, reaction 14, the internal excitation of $HCFOH(OH_2)^+$ is sufficient to permit rearrangement and dissociation, eq. 16, yielding $HFH(OH_2)^+$

$$HCFOH(OH_2)^+ \rightarrow HFH(OH_2)^+ + CO \quad (16)$$

through loss of CO. The proton bound complex of hydrogen fluoride and water in reaction 16 is one of the two new minor ions observed in this system. $HFH(OH_2)^+$ decays via hydrated proton transfer to H_2O, reaction 17. The second new minor ion observed in this experiment is

$$HFH(OH_2)^+ + H_2O \rightarrow H(OH_2)_2 + HF \quad (17)$$

protonated fluoroformate, $HCFOH^+$. The source of $HCFOH^+$ is less clear, however. Double resonance indicates H_3O^+ is the only likely precursor for this ion. Because $HCFOH^+$ exists only at very short times, it may be due to reaction of excited H_3O^+ as in eq. 18 which is endothermic. This seems reasonable because excited H_3O^+ is observed in water following electron impact.[48,49] After thermalization, $HCFOH^+$

$$(H_3O^+)^* + (CF_2H)_2O \rightarrow HCFOH^+ + H_2O + CF_3H \qquad (18)$$

then decays via exothermic proton transfer to the stronger base H_2O, eq. 19. Rates observed in mixtures yielding $H(OH_2)_2^+$ are presented in Table I.

$$HCFOH^+ + H_2O \rightarrow H_3O^+ + HCFO \qquad (19)$$

Hydrated proton transfer reactions, acetic acid as an example. Ion-molecule reactions shown in Figure 4 are observed in a 1:2.8:24 mixture of CH_3COOH, $(CF_2H)_2O$, and H_2O. Only species present after 400 msec are depicted. At shorter time the chemistry which produces $H(OH_2)_2^+$ dominates but has been omitted for clarity. Intensities of these ions are negligible after 400 msec and are not included in the normalization of Figure 4. Double resonance ejection experiments confirm that $H(OH_2)_2^+$ transfers a hydrated proton to acetic acid, eq. 20, yielding the proton bound complex $CH_3COOH_2(OH_2)^+$. In 10% of these encounters, however, the product ion is $CH_3COOH_2^+$, eq. 21, though most of the $CH_3COOH_2^+$ present is due to direct proton transfer from H_3O^+ at shorter times, eq. 22. Equation 20 is a specific example of the process generalized in eq. 6. Equation 21 is generalized in eq. 23.

TABLE I: Rate Constants for Reactions in Sequences Yielding $H(OH_2)_2^+$

Reaction	k[a]
$H_3O^+ + CH_3CHCl_2 \xrightarrow{60\%} CH_3CHClOH_2^+ + HCl$	16[b]
$\xrightarrow{40\%} CH_3CHOH^+ + 2HCl$	
$CH_3CHClOH_2^+ + H_2O \rightarrow H(OH_2)_2^+ + CH_2CHCl$	14[b]
$H_3O^+ + CH_3CHBr_2 \xrightarrow{60\%} CH_3CHBrOH_2^+ + HBr$	14[b]
$\xrightarrow{40\%} CH_3CHOH^+ + 2HBr$	
$CH_3CHBrOH_2^+ + H_2O \rightarrow H(OH_2)_2^+ + CH_2CHBr$	16[b]
$H_3O^+ + CH_3CHF_2 \xrightarrow{60\%} CH_3CHFOH_2^+ + HF$	29[c]
$\xrightarrow{40\%} CH_3CHOH^+ + 2HF$	
$CH_3CHFOH_2^+ + H_2O \rightarrow H(OH_2)_2^+ + CH_2CHF$	13 ± 10[d]
$H_3O^+ + (CF_2H)_2O \rightarrow HCFOHOH_2^+ + CF_3H$	11.5[e]
$HCFOHOH_2^+ + H_2O \rightarrow H(OH_2)_2^+ + HCFO$	
$CF_2H^+ + (CF_2H)_2O \rightarrow CF_2HOCFH^+ + CF_3H$	18.0[e]
$CF_2HOCFH^+ + H_2O \rightarrow CF_2HOH_2^+ + HCFO$	7.7[f]
$CF_2HOH_2^+ + H_2O \rightarrow H(OH_2)_2^+ + CF_2$	

[a] Units are kcal mol^{-1}.

[b] Ref. 33.

[c] The rate constant is independent of pressure, but the branching ratio is not, see text.

[d] Because of mass degeneracies, this rate constant is difficult to measure.

Table I (continued)

[e]This work.

[f]The system is extremely complicated so that accurate estimates of the rate for decay of a secondary ion are difficult to obtain.

FIGURE 4. Variation of ion abundance with time following a 20 msec, 70.0 eV electron beam pulse in a 1:2.8:24 mixture of CH_3COOH, $(CF_2H)_2O$, and H_2O at a total pressure of 2.5×10^{-6} torr. Ions involved in the initial production of $H(OH_2)_2^+$ are omitted for clarity. Concentrations of these species are negligible after 400 msec and are not included in the normalization.

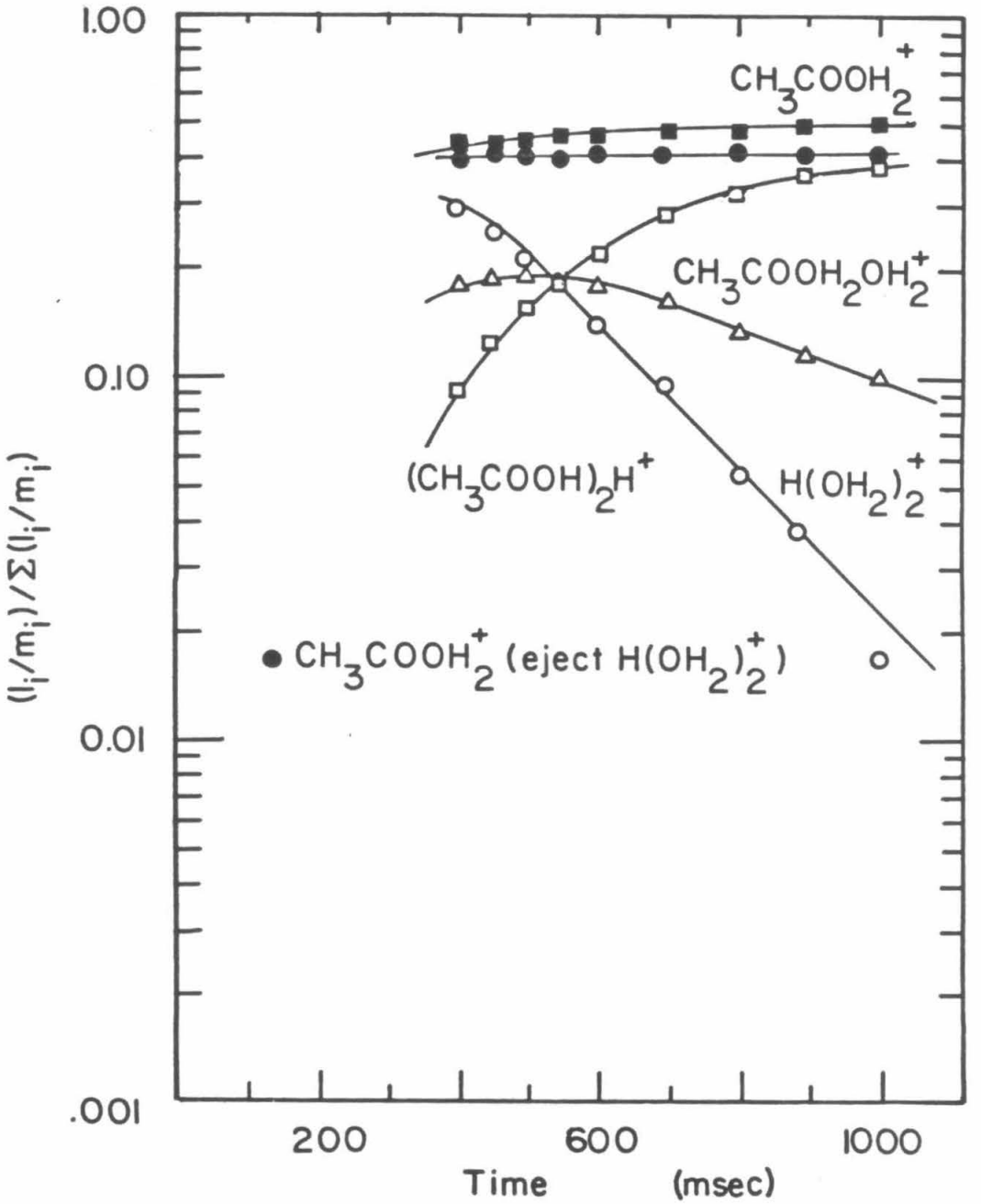
1.00
0.10
0.01
.001
200
600
1000
Time (msec)
$(I_i/m_i)/\Sigma(I_i/m_i)$
$CH_3COOH_2^+$
$CH_3COOH_2OH_2^+$
$(CH_3COOH)_2H^+$
$H(OH_2)_2^+$
● $CH_3COOH_2^+$ (eject $H(OH_2)_2^+$)

$$H(OH_2)_2^+ + CH_3COOH \xrightarrow{90\%} CH_3COOH_2(OH_2)^+ + H_2O \quad (20)$$

$$H(OH_2)_2^+ + CH_3COOH \xrightarrow{10\%} CH_3COOH_2^+ + 2(H_2O) \quad (21)$$

$$H_3O^+ + CH_3COOH \rightarrow CH_3COOH_2^+ + H_2O \quad (22)$$

Reaction 23 is only observed for bases with proton affinities greater

$$H(OH_2)_2^+ + B \rightarrow BH^+ + 2(H_2O) \quad (23)$$

than PH_3. The competition between proton transfer and hydrated proton transfer from $H(OH_2)_2^+$ is the subject of a subsequent paper.[50] The only other species present after 400 msec is $(CH_3COOH)_2H^+$ produced via solvated proton transfer, eq. 24.

$$CH_3COOH_2(OH_2)^+ + CH_3COOH \rightarrow (CH_3COOH)_2H^+ + H_2O \quad (24)$$

Solvated proton transfer in 3 and 4 component mixtures. When small concentrations of a Lewis base, B, are added to mixtures containing $(CF_2H)_2O$ and H_2O, the product complex $BH(OH_2)^+$ produced via eq. 6 is observed, as in the case of B = CH_3COOH above. If the base contains oxygen, eq. 7 is observed to yield BHB^+ as well. Thus three-component mixtures containing H_2O, an organohalide precursor of $H(OH_2)_2^+$, and one of a series of Lewis bases were examined for the presence of $BH(OH_2)^+$ and BHB^+ produced via eqs. 6 and 7 respectively. In order to avoid mass degeneracies among the ions of interest, mixtures containing CH_3CHCl_2, CH_3CHF_2 or $(CF_2H)_2O$ each had to be employed in separate cases. Table II lists rate constants measured for these

TABLE II: Measured Rate Constants for Solvated Proton Transfer

B	PA(B)[a]	k_1[b]	$\Delta H^\circ_{r_1}$[b]	k_2[b]	ΔH_{r_2}[b]
H_2O	174		0		0
H_2S	177.6	not observed	11.7[c]		
			6.7[d]		
HCN	178.2	15.5	-0.95[e]	not observed	-0.3[f]
		1.0[g]			
H_2CO	178.3	12.0[e]	-0.16[e]	16.0	-0.8[h]
		30 ± 20[j]	-0.41[h]		
CF_2HCH_2OH	181.6	17.7		6.8	
HCOOH	183.8	17.3		9.0	
		24 ± 7[j]			
C_6H_6	185.1	not observed			
CH_3OH	185.9	20.5		10.1	
		24 ± 6[j]			
CH_3CHO	188.7	15.0		20.0	
		31 ± 8[j]			
CH_3SH	189.6	18.9		not observed	
CH_3CH_2OH	190.4	25 ± 6[j]			
PH_3	191.1	13.1		not observed	
CH_3COOH	191.7	12.1	-6.5[k]	13.7	
		27 ± 8[j]			
$C_6H_5CH_3$	192.4	not observed			
$(CH_3)_2O$	193.8	18.6	-9.4[k]	9.1	-6.8[l]
		22 ± 6[j]			

TABLE II. (continued)

B	PA(B)[a]	k_1[b]	$\Delta H^\circ_{r_1}$[b]	k_2[b]	ΔH_{r_2}[b]
$O\text{-}C_6H_4(CH_3)_2$	194.8	not observed			
$(CH_3)_2S$	201.3	<0.01		not observed	
CH_2PH_2	205.5	<0.01		not observed	
NH_3	206	not observed	-16.2[k]		-5.0[m]
		20 ± 4[j]		12[m]	

[a]Units are kcal mol^{-1}. Values from ref. 35 assuming $PA(NH_3)$ = 206 ± 2 kcal mol^{-1} from Houle, F. A.; and Beauchamp, J. L. J. Am. Chem. Soc. 1979, 101, 4067.

[b]Units for measured rate constants are 10^{-10} cm^3 $molecule^{-1}$ sec^{-1}. These should be accurate to ±20%. Units for enthalpies of reaction are kcal mol^{-1} and refer to 298° K. The subscript 1 refers to the process: $H(OH_2)_2^+ + B \rightarrow BH(OH_2)^+ + H_2O$. The subscript 2 refers to the process: $BH(OH_2)^+ + B \rightarrow HB_2^+ + H_2O$. Unless specified, results are from this work.

[c]Ref. 19.

[d]Ref. 29.

[e]Ref. 33.

[f]Ref. 26.

[g]Ref. 11.

[h]Ref. 2.

[j]Ref. 28.

[k]Ref. 32.

[l]Ref. 25.

[m]Ref. 1.

processes. Other rate constants, proton affinities, and enthalpies of reaction derived in related studies are also presented.

A series of four component mixtures were generated by adding a second Lewis base to the three component mixtures discussed. The complexes $B_1H(OH_2)^+$ and $B_2H(OH_2)^+$ are generated in these systems via eq. 6.

Unfortunately, because exothermic proton transfer from H_3O^+ to each base present, eq. 25, competes with production of $H(OH_2)_2^+$ only

$$H_3O^+ + B \rightarrow BH^+ + H_2O \qquad (25)$$

minimal concentrations of bases can be added to these mixtures before the desired solvated proton transfer chemistry is severely curtailed. For this reason, equilibrium solvated proton transfer was not observed because pressures were too low to permit a sufficient number of collisions to occur so that equilibrium could be established over the time scale of the experiment. However, the relative stability of $B_1H(OH_2)^+$ and $B_2H(OH_2)^+$ could be determined from the preferred direction of hydrated proton transfer, eq. 5, between these species. A summary of systems studied and results obtained is presented in Table III.

IV. Discussion

Reactions that generate $H(OH_2)_2^+$. Both proton bound complexes of species less basic than water, and protonated α-halo-alcohols dominate the chemistry of $H(OH_2)_2^+$ production. In mixtures of H_2O and $(CF_2H)_2O$, initial encounters between H_3O^+ and $(CF_2H)_2O$ yield the proton bound complex of HCFO and H_2O, eq. 14.[40] A fraction of these $HCFOH(OH_2)^+$

TABLE III. A Summary of H_3O^+ Transfer Reactions Investigated.[a]

PA		B_1	B_2HW^+	H_2SHW^+	H_2OHW^+	H_2COHW^+	$HCNHW^+$	$CH_3SH_2W^+$	$CF_2HCH_2OH_2W^+$	PH_4W^+	$HCOOH_2W^+$	$CH_3OH_2W^+$	CH_3CHOHW^+	$CH_3COOH_2W^+$	$(CH_3)_2SHW^+$	$(CH_3)_2OHW^+$	$CH_3PH_3W^+$
177.6	Neutral Base Reactant	H_2S															
174		H_2O	E														
178.3		H_2CO	E	E													
178.2		HCN	E	E	E												
189.6		CH_3SH	O	+	O	+											
181.6		CF_2HCH_2OH	O	+	+	+	+										
191.1		PH_3	O	+	O	O	O	+									
183.8		HCOOH	O	+	O	O	O	O	+								
185.9		CH_3OH	O	+	O	O	O	+	+	?							
188.7		CH_3CHO	O	+	O	O	O	O	+	+	C						
191.7		CH_3COOH	E	+	E	E	O	O	+	O	O	C					
201.3		$(CH_3)_2S$	O	+	O	O	O	+	+	+	O	O	+				
193.8		$(CH_3)_2O$	E	+	E	E	O	O	O	O	O	O	E	P			
205.5		CH_3PH_2	O	+	O	O	O	O	O	O	O	P	P	O	O		

[a]The reaction investigated is $B_1 + B_2HW^+ \rightarrow B_2 + B_1HW^+$ where $W = H_2O$.
Notation in the table is as follows:

+ indicates reaction is observed in the forward direction only.

E indicates reaction will be spontaneous based on thermochemical results obtained in earlier studies.

? indicates a mass degeneracy hampered confirmation of this reaction.

TABLE III. (Continued)

C indicates the product of this reaction is $B_1HB_2^+$ exclusively so direction of H_3O^+ transfer could not be determined.

P indicates double resonance results were not conclusive due to lack of intensity of ions involved. However, indirect evidence such as changes in the relative intensities of each complex as a function of base pressure suggests that the forward reaction is spontaneous.

O indicates system not studied.

ions retain sufficient excess energy to rearrange and eliminate CO forming another proton bound complex, $HFH(OH_2)^+$, eq. 16. Figure 5 depicts a potential energy diagram for production of these two complexes, $HCFOH(OH_2)^+$ and $HFH(OH_2)^+$. In Fig. 5, the thermochemistry of neutral fluorinated species were approximated from the additivity tables of Bensen[51] due to the lack of experimental values for these quantities. Proton affinities and hydration enthalpies were extrapolated from values of related species.[32,39] Allowing for errors of ± 10 kcal $mole^{-1}$, reaction 16 still appears to be exothermic. Since this rearrangement is observed, the activation barrier for reaction 16 must be smaller than the total internal energy available to $HCFOH(OH_2)^+$. Based on Fig. 5, $HCFOH(OH_2)^+$ can be formed via reaction 14 with a maximum of 29 kcal $mole^{-1}$ excess internal energy. Thus the enthalpy of activation for elimination of CO from this complex should be somewhat less than 28 kcal $mole^{-1}$. Once generated, both $HCFOH(OH_2)^+$ and $HFH(OH_2)^+$ transfer a solvated proton to H_2O yielding $H(OH_2)_2^+$, eqs. 15 and 17, respectively.

Dependent upon the structure assumed for the ion CF_2HOCFH^+, two mechanistic schemes have been advanced for the process ultimately yielding $H(OH_2)_2^+$ that begins with this species.[40] Distinguishing between these two pathways was not attempted in this study. CF_2HOCFH^+ is either a proton bound complex of CF_2 and HCFO, structure I, or a delocalized onium ion, structure II.[40] Beginning with I, the product of

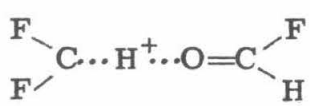

I

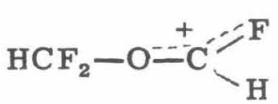

II

FIGURE 5. Energetics of formation of $HFH(OH_2)^+$ from H_3O^+ and $(CF_2H)_2O$. Neutral heats of formation were derived from additivity tables, ref. 51. Proton affinities and hydration enthalpies were estimated from values for similar species listed in refs. 32 and 39.

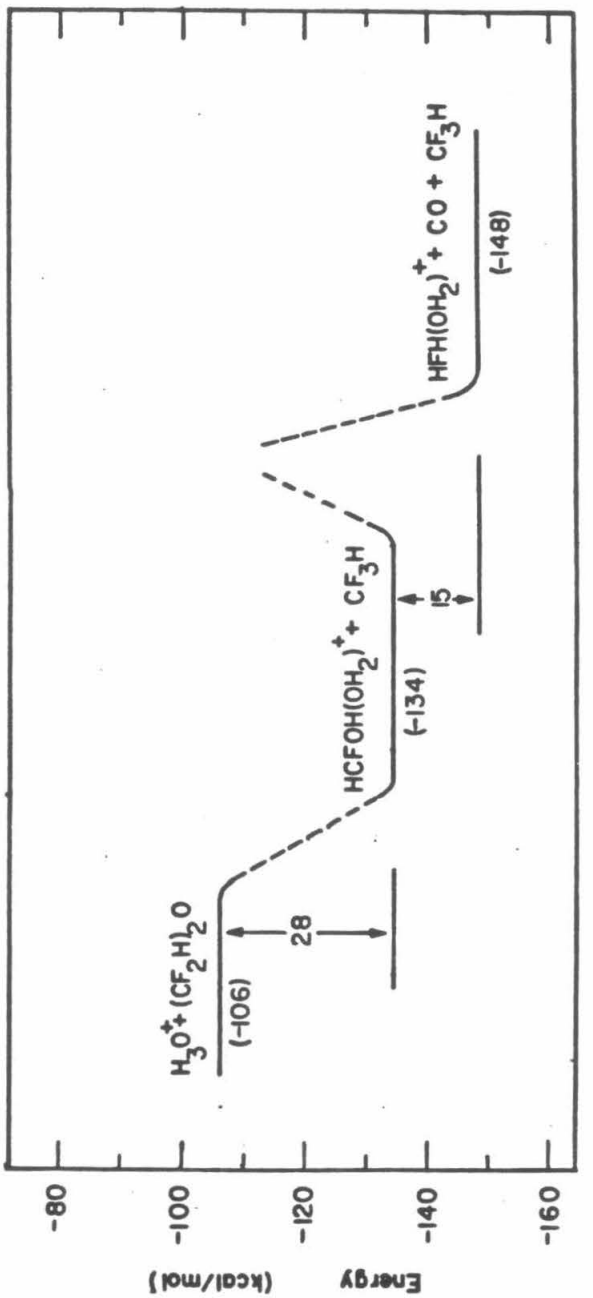
-80
-100
-120
-140
-160
Energy (kcal/mol)
$H_3O^+(CF_2H)_2O$
(-106)
28
$HCFOH(OH_2)^+ + CF_3H$
(-134)
15
$HFH(OH_2)^+ + CO + CF_3H$
(-148)

reaction 12, $CF_2HOH_2^+$, would be the proton bound complex of CF_2 and H_2O. A second solvated proton transfer, reaction 13, then yields $H(OH_2)_2^+$. However, if II is the actual strcture for CF_2HOCFH^+, the product of reaction 12 is a protonated α,α-difluoromethyl alcohol. This intermediate is similar to the protonated α-haloethyl alcohols proposed in mixtures of CH_3CHCl_2 or CH_3CHBr_2 with H_2O.[33,45] Since the intermediates in mixtures of CH_3CHF_2 and H_2O also parallel those in the other dihaloethane systems, it is instructive to compare the energetics of $H(OH_2)_2^+$ production from protonated α,α-difluoromethyl alcohol with production from protonated α-fluoromethyl alcohol as presented in Fig. 6. Thermochemical quantities for Fig. 6 were estimated as in Fig. 5.[32,39,45,51]

In a mixture of CH_3CHF_2 and H_2O, once H_3O^+ reacts via eq. 9 to yield protonated α-fluoroethyl alcohol, production of both CH_3CHOH^+ via eq. 10 and $H(OH_2)_2^+$ via eq. 11 is energetically accessible, Fig. 6. In contrast, $H(OH_2)_2^+$ is the sole product at long times in mixtures of $(CF_2H)_2O$ and H_2O because, unlike the analogous reaction 10, loss of HF from protonated α,α-difluoromethyl alcohol is endothermic. Interestingly, formation of $HCFOH^+$ from the proton bound complex of CF_2 and H_2O is also expected to be endothermic. Therefore, $H(OH_2)_2^+$ would be the sole product at long times from either mechanism in $(CF_2H)_2O$ and H_2O, Fig. 6.

A further note concerning reactions between H_3O^+ and CH_3CHF_2 is included because of its significance regarding nucleophilic displacement in the gas phase. It has been suggested that two conditions must be met for nucleophilic displacement to be observed in the ICR.[14,15,43,52]

FIGURE 6. Energetics of intermediates in the formation of $H(OH_2)_2^+$. Species present in mixtures of CH_3CHF_2 and H_2O are presented in the upper portion of the figure. Species in the lower portion occur in mixtures containing $(CF_2H)_2O$ and H_2O. Neutral heats of formation were derived from additivity tables, ref. 51. Proton affinities and hydration enthalpies were estimated from values for similar species listed in refs. 32 and 39.

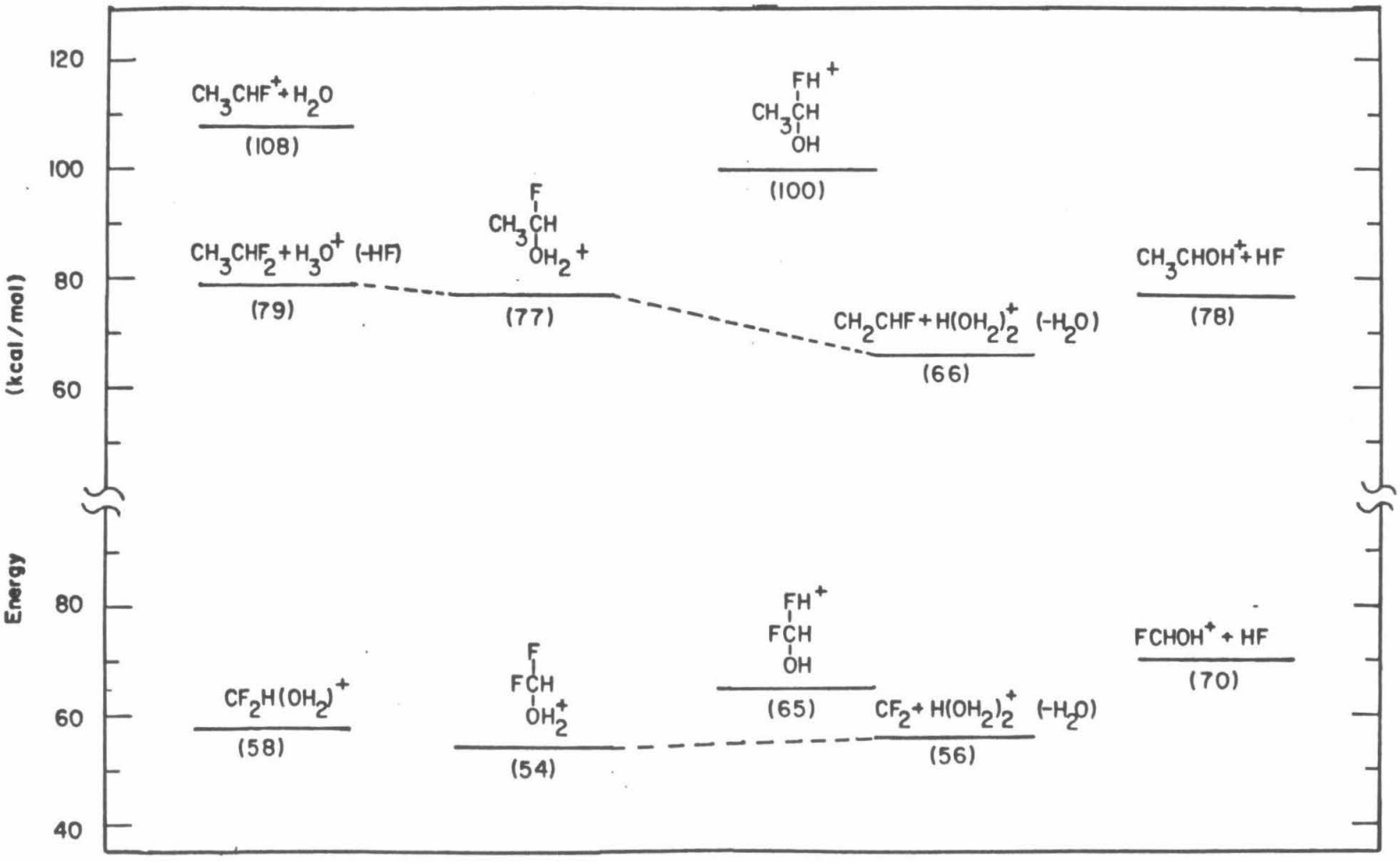
Energy (kcal/mol)
120
100
80
60
80
60
40
$CH_3CHF^+ + H_2O$
(108)
$CH_3CHF_2 + H_3O^+$ (-HF)
(79)
$CH_3\overset{F}{\underset{}{C}}H\overset{}{\underset{OH_2^+}{}}$
(77)
$CH_3\overset{FH^+}{\underset{}{C}}H\overset{}{\underset{OH}{}}$
(100)
$CH_2CHF + H(OH_2)_2^+$ (-H_2O)
(66)
$CH_3CHOH^+ + HF$
(78)
$CF_2H(OH_2)^+$
(58)
$F\overset{}{\underset{}{C}}H\overset{}{\underset{OH_2^+}{}}$
(54)
$F\overset{FH^+}{\underset{}{C}}H\overset{}{\underset{OH}{}}$
(65)
$CF_2 + H(OH_2)_2^+$ (-H_2O)
(56)
$FCHOH^+ + HF$
(70)

Supplemental to the requirement that the overall reaction be exothermic, it was suggested that proton transfer from the substrate to the nucleophile must be endothermic. Based on trends in the proton affinity of halogenated species and, more specifically, the effects of fluorine substitution,[39] the proton affinity of the nucleophile H_2O is expected to be at least 5 kcal $mole^{-1}$ greater than the CH_3CHF_2 substrate. Yet the nucleophilic displacement reaction 9 is observed. It would seem that rules governing the observation of nucleophilic displacement in the gas phase at low pressure are more complicated than originally suggested.

Periodic Trends in the Energetics of Hydration. Relative H_3O^+ affinities for the Lewis bases examined in this study can be derived from the list of observed hydrated proton transfer reactions presented in Table III. Consistent with the set of reactions observed, H_3O^+ affinities increase in the following order: $H_2S < H_2O < H_2CO < HCN < CH_3SH < CF_2HCH_2OH < PH_3 < HCOOH < CH_3COOH < (CH_3)_2S < (CH_3)_2O$. With two omissions, this list is simply a reproduction of the vertical column of Table III. The two omissions are CH_3OH and CH_3CHO. Because $HCOOH_2OH_2^+$ and $(CH_3OH)_2N^+$ are ions of the same mass, relative H_3O^+ affinities between HCOOH and CH_3OH could not be determined. Further, since CH_3OH, CH_3CHO, and CH_3COOH tend to solvate each other to the exclusion of H_2O (reaction 7 occurs exclusively rather than reaction 5) so that relative H_3O^+ affinities could not be determined among CH_3OH, CH_3CHO, and CH_3COOH. Viewed in conjunction with other results, however, these problems can be overcome and the data can be made more quantitative.

Due to the nature of our experiment, the monitoring of transfer between hydrated protons, relative H_3O^+ affinities are measured. The relationship between H_3O^+ affinities $D(B-HOH_2^+)$ for a base, and H_2O affinities $D(BH^+-OH_2)$ for the corresponding conjugate acid is presented in Scheme I.

Scheme I

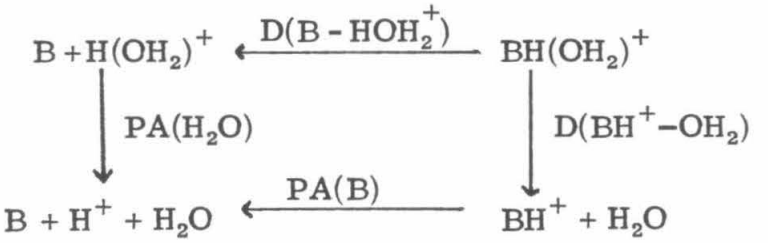

Thus, $D(B-HOH_2^+)$ and $D(BH^+-OH_2)$ are related by the difference in proton affinities between base and water, eq. 26. By plotting $D(BH^+-OH_2)$ calculated using eq. 25 as a function of $PA(B) - PA(H_2O)$, Fig. 7, results presented in Table II can be considered with respect to the inverse relationship between proton affinity and H_2O affinity discussed by Kebarle et al.[32]

In Figure 7, H_2O affinities for bases represented by filled circles have been determined independently.[25, 29, 32, 33] Bases studied in this work are represented by vertical lines signifying the uncertainty in $D(BH^+-OH_2)$ as follows. From Table III: CF_2HCH_2OH, HCOOH, CH_3OH, CH_3CHO, CH_3SH, and PH_3 all lie between HCN, $D(B-HOH_2^+)$ = 33.9 kcal mol^{-1},[33] and CH_3COOH, $D(B-HOH_2^+)$ = 39.5 kcal mol^{-1}.[32] Thus, $D(BH^+-OH_2)$ for each of these bases must lie between limits calculated from $D(B-HOH_2^+)$ for HCN and CH_3COOH using Scheme I. This repre-

FIGURE 7. Relationship between the hydration energy, $D(BH^+\cdots OH_2)$, and the proton affinity of B relative to H_2O, $PA(B) - PA(H_2O)$ (see ref. 33): but $PA(H_2O) = 174$ kcal mol^{-1} and $PA(NH_3) = 206$ kcal mol^{-1}. Dotted lines represent limits imposed on the uncertainty of these values from observed reactions with other species for which $D(BH^+\cdots OH_2)$ has been independently determined. (Such species are represented by filled circles in the figure.) Filled squares and open circles represent two sets of $D(BH^+\cdots OH_2)$ estimates for species addressed in this study. Filled squares are generated assuming equal uncertainty for all species while open circles are generated by assuming all O containing bases lie on the plotted curve, see text.

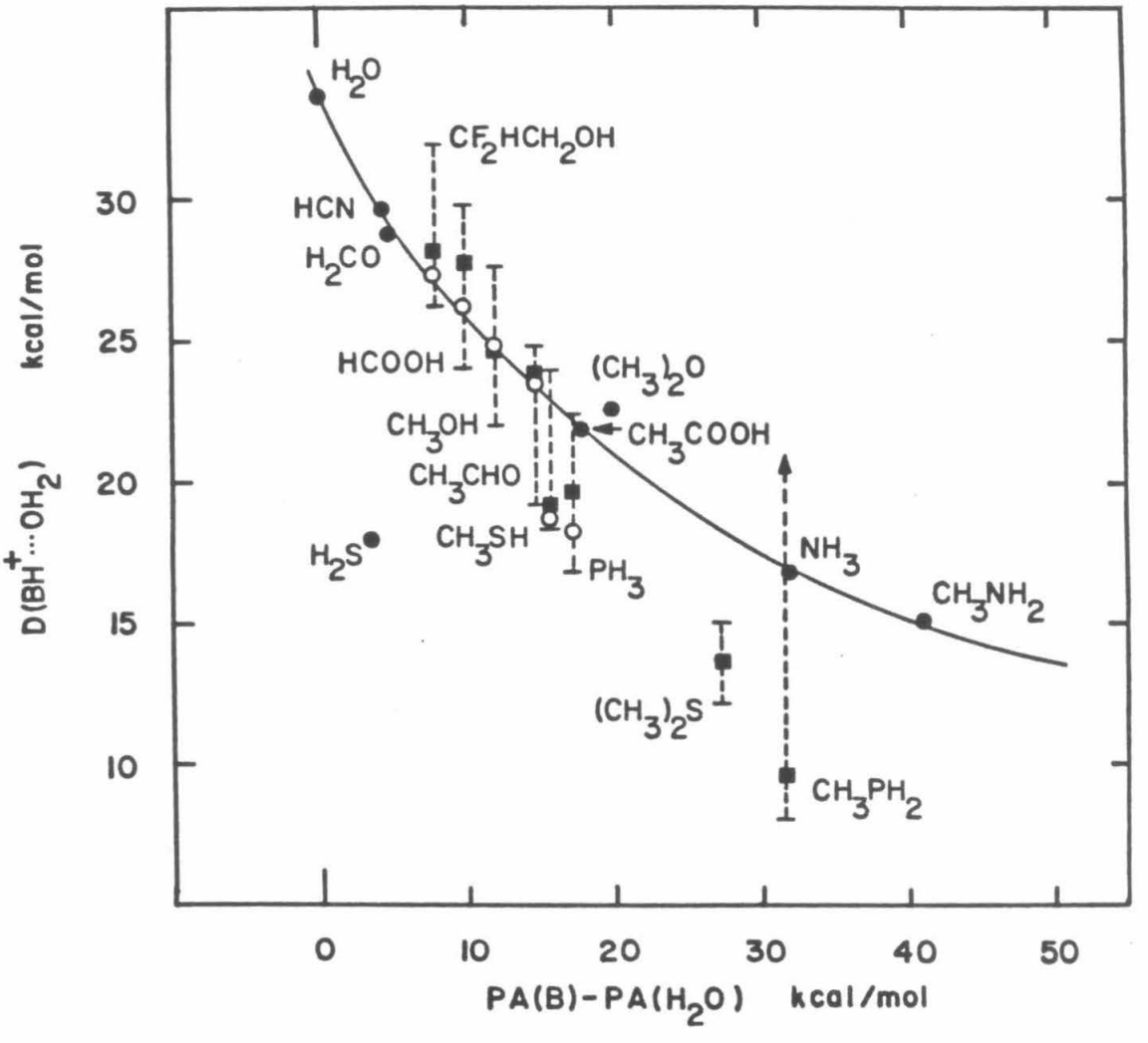
H_2O
CF_2HCH_2OH
HCN
H_2CO
HCOOH
$(CH_3)_2O$
CH_3OH
CH_3COOH
CH_3CHO
H_2S
CH_3SH
PH_3
NH_3
CH_3NH_2
$(CH_3)_2S$
CH_3PH_2
30
25
20
15
10
0
10
20
30
40
50
$D(BH^+\cdots OH_2)$ kcal/mol
$PA(B)-PA(H_2O)$ kcal/mol

sents a spread of 5.6 kcal mol^{-1}. Since the relative $D(B\text{-}HOH_2^+)$ between most of these bases have been determined, however, it should be possible to narrow such limits. Assuming, in the absence of additional data, that the five bases known to span this 5.6 kcal mol^{-1} gap are equally spaced, the distribution represented by the open squares in Fig. 7 is generated from $D(B\text{-}HOH_2^+)$ of $HCN < CH_3SH < CF_2HCH_2OH < PH_3 < HCOOH < CH_3CHO < CH_3COOH$. In this case the oxygen containing bases lie close to the correlation curve, while CH_3SH and PH_3 are lower. Alternatively, assuming the oxygen containing bases should lie on the correlation line and spacing all other bases accordingly, the distribution represented by the open circles is derived. Again CH_3SH and PH_3 lie well below the line. This is reasonable considering that H_2S is known to lie below the curve.[25] Looking at other bases presented, $(CH_3)_2S$ is bounded by CH_3COOH[32] and $(CH_3)_2O$,[29] Table III, and lies below the correlation curve, as well. Unfortunately, no upper bound for CH_3PH_2 was conclusively determined because only minute quantities of the hydrated species could be produced.

Comparing proton affinities in the vertical column of Table III, it is immediately apparent that H_2S, CH_3SH, PH_3 and $(CH_3)_2SH$, are anomalous. This anomaly is also obvious in Fig. 7 where all of these species lie below the progression of other bases. Thus bases with heteroatoms of second-row elements are more weakly bound to H_3O^+ than O or H bases with similar proton affinities. Decreased stability of complexes containing n-donor bases with second-row heteroatoms will be considered in the next section.

A Simple Model of Hydrogen Bonding in $BH(OH_2)^+$ Complexes. The relationship between H_3O^+ affinities and H_2O affinities presented in Scheme I illustrates that proton bound complexes, $BH(OH_2)^+$ possess two low energy pathways to decomposition yielding either B and H_3O^+ or BH^+ and H_2O. Thus, any description of bonding in these species must incorporate two configurations resembling both protonated water solvated by the Lewis base B, $B\cdots HOH_2$, and the conjugate acid of B solvated by water, $BH^+\cdots OH_2$. Stabilization in each configuration should be largely due to electrostatic interactions.[19,20] Covalent contributions will only be important when the energy of the two configurations are nearly equivalent. For example, a large covalent bonding component is expected in the symmetric case, $H(OH_2)_2^+$,[20,32] because mixing of two configurations is greatest when they are degenerate. However, as the proton affinity of B is increased between to H_2O, so that the two configurations are no longer degenerate, the significance of covalent contributions decreases rapidly. In all of the complexes examined in this study, $PA(B) > PA(H_2O)$. Thus bonding in $BH(OH_2^+)$ will be dominated by contributions from $BH^+\cdots OH_2$ because the proton should associate preferentially with the stronger base B. Unless the difference is proton affinities is large, however, stability of $BH(OH_2)^+$ will be due to a combination of contributions from both configurations.

Since stabilization in each configuration results principally from electrostatic interactions, it is instructive to assess factors affecting such phenomena. Generally, larger dipole moments and polarizabilities of B lead to greater accomodation of the partial charge on the proton

bound to H_2O so that $B\cdots HOH_2^+$ will be stabilized. At the same time, a greater partial charge on the proton of the conjugate acid of B will lead to more favorable interactions with H_2O stabilizing $BH^+\cdots OH_2$. Viewing hydrogen bonding as a composite of configurations in this manner facilitates an understanding of periodic trends in the stabilities of cluster formation observed in this study.

Best estimates of $D(BH^+\text{-}OH_2)$ and $D(B\text{-}HOH_2^+)$ for the series of bases examined in this work are presented in Table IV. Error limits can be found in Fig. 7 and related discussion. The quantity $D(BH^+\text{-}OH_2)$ represents the least endothermic path for dissociation of all complexes presented. Therefore, H_2O affinities present a reasonable measure of relative stabilities for such species. Available proton affinities, dipole moments, and polarizabilities for the various n-donor bases are included as well. First ionization energies are presented for each base only to suggest that the lack of any apparent trend among these values in Table IV would make a qualitative molecular orbital model for such complexes difficult to assess. Decreased stability in $BH(OH_2)^+$ complexes incorporating second-row heteroatoms can be understood as follows. Contributions from $BH^+\cdots OH_2$ should dominate bonding in these complexes because $PA(B) > PA(H_2O)$ for all species listed. Since the stability of this configuration is directly related to the density of charge on the proton of BH^+ and partial charges on the protons of PH_4^+ and H_3S^+ are small relative to NH_4^+ and H_3O^+,[53] bonding in complexes containing PH_3 and H_2S should be weaker than those of NH_3 or H_2O as observed. Methyl substitution tends to increase basicity and decrease the density of charge on protons of conjugate acids.[32,53] The partial

TABLE IV. A Comparison of Binding Energies to Several Reference Acids Including H^+, Li^+, and H_3O^+ for Bases Studied in This Work.[a]

B	$D(B\text{-}H^+)$[b]	$D(B\text{-}Li^+)$[c]	$D(B\text{-}HOH_2^+)$[d]	$D(BH^+\text{-}OH_2)$[e]	μ[f]	α[g]	1st. ionization energies[h]
H_2S	177.6		21.6	18	0.97	3.88	10.47
H_2O	174	34.0	33	33	1.85	1.45	12.62
H_2CO	178.3	36.0	33.2	28.9	2.33	2.81	10.88
HCN	178.2	36.4	33.9	29.7	2.98	2.59	13.59
CH_3SH	189.6	31.8	(34)	(18.5)	1.52	5.72	9.44
CF_2HCH_2OH	181.6		(34.5)	(27)			
PH_3	191.1		(35)	(18)	0.58		9.98
HCOOH	183.8		(35.5)	(25.5)	1.41		11.33
C_6H_6	185.1	36.6	<33	<22	0	8.61	9.25
CH_3OH	185.9	38.1	(37)	(25)	1.70	3.25	10.85
CH_3CHO	188.7	41.3	(38)	(23)	2.69	4.53	10.23
CH_3COOH	191.7		39.5	21.9	1.74		10.35
$C_6H_5CH_3$	192.4		<33	<15			8.82
$(CH_3)_2S$	201.3	32.8	(41)	(13.5)	1.50	7.56	8.69
CH_3PH_2	205.5		>39.5	>8	1.10		9.72

TABLE IV. (Continued)

B	$D(B\text{-}H^+)^b$	$D(B\text{-}Li^+)^c$	$D(B\text{-}HOH_2^+)^d$	$D(BH^+\text{-}OH_2)^e$	μ^f	α^g	1st. ionization energies[h]
$(CH_3)_2O$	193.8	39.5	42.4	22.6	1.30	5.24	9.96
$O\text{-}C_6H_4(CH_3)_2$	194.8		<33	<12			8.58
NH_3	206	39.1	49.2	17.2	1.47	2.16	10.17

[a]Units are kcal mol^{-1} except as noted.

[b]$D(B\text{-}H^+) \equiv PA(B)$. Values are from Ref. 35 assuming $PA(NH_3) = 206 \pm 2$ kcal mol^{-1} from Houle, F. A.; and Beauchamp, J. L. J. Am. Chem. Soc. 1979, 101, 4067.

[c]Values are from Ref. 37 except as noted.

[d]Values are calculated from $A(H_2O)$ using Scheme I.

[e]Values are taken from Table II or constitute best estimates extrapolated from Fig. 7. Extrapolations are in parentheses.

[f]Dipole moments are expressed in debyes. Values are from Weast, R. C., ed.; "Handbook of Chemistry and Physics," 53 ed.; Chem.Rubber Co., Cleveland, 1972, P.E-51.

[g]Polarizabilities are expressed in $Å^3$. Values are calculated as described in Adamson, A. W.; "A textbook of Phys. Chem." Academic Press, New York, 1973; p. 88-90.

[h]Units are eV. Values are from Rosenstock, H. M.; Draxl, K.; Steiner, B. W.; and Herron, J. T., J. of Phys. Chem. Ref. Data, 1977, 6, suppl. 1.

charge does not appear to change appreciably with methyl substitution, however, because symmetric proton bound dimer association energies are approximately constant for a number of oxygen containing bases over a large range of proton affinities,[24,54] and hydrogen bond strengths of symmetric dimers are linearly related to the density of charge surrounding protons of respective conjugate acids.[19] Thus all complexes containing S and P bases should exhibit weaker bonding than O and N bases with comparable proton affinities.

Though H_2O affinities of H_2S, CH_3SH, and PH_3 are lower than O and N bases with similar proton affinities, all three values are comparable to the H_2O affinity of NH_3. Since contributions from $BH^+\cdots OH_2$ should favor NH_3, the configuration $B\cdots HOH_2^+$ must be important for $H_2SH(OH_2)^+$, $CH_3SH_2(OH_2)^+$, and $PH_4(OH_2)^+$. This is reasonable because the proton affinities of S and P bases are much lower than NH_3 so that $B\cdots HOH_2^+$ should be relatively more important. In addition, greater polarizabilities for S and P species allow a more favorable electrostatic interaction between B and H_3O^+ with respect to analogous O or N bases suggesting that $B\cdots HOH_2^+$ should confer relatively greater stabilization to $BH(OH_2)^+$ complexes containing S or P species. However, since the proton affinities of $(CH_3)_2S$ and CH_3PH_2 are much higher, approaching that of NH_3, contributions from $B\cdots HOH_2^+$ decrease and the H_2O affinities for these species are small.

The inability to detect $BHOH_2^+$ complexes for the three substituted benzenes included in this work may further support the above model, though a negative result does not prove that H_2O affinities for these species are as low as suggested in Table IV because there may be a

kinetic problem associated with formation of complexes containing these species. However, these results concur with earlier studies where alkyl substituted benzenes are shown to protonate on the ring and do not form hydrated species in condensation reactions at higher pressures.[36] Protonation of substituted benzenes yield a cation with charge delocalized principally at three sites on the ring ortho and para to the site of protonation.[36] For all three conjugate acids, therefore, partial charge at proton sites is expected to be very small and stabilization from $BH^+\cdots OH_2$ should be weak. Thus, protonated alkyl substituted benzenes are not expected to bond strongly to H_2O and no $BH(OH_2)^+$ complexes have been observed in this or related work.[36]

Trends in proton affinities, lithium ion affinities and H_3O^+ affinities. Available lithium ion affinities are presented along with proton affinities, H_3O^+ affinities, and the other data presented in Table IV. Unlike proton or lithium ion affinities, which represent interaction of a single atomic cation with a single electron lone pair of a base, H_3O^+ affinities represent formation of a complex multi-center bond. The two-configuration model discussed in this work suggests that bonding in $BH(OH_2)^+$ represents a proton shared by two electron lone pairs located on separate base sites yielding a three-center-four-electron bond. Molecular orbital considerations and other models of these species also characterize bonding in $BH(OH_2)^+$ complexes as delocalized over several nuclear centers.[18-24, 32] For this reason, comparisons of H_3O^+ affinities with proton or lithium ion affinities must be made with extreme care.

Comparison of H_3O^+ affinities and proton affinities show reasonable correlation in Table IV, with the exception of bases containing heteroatoms of the second row. Interestingly, lithium ion affinities also seem to show a second row effect. Lithium ion affinities are weaker for S containing bases than O or N bases with similar proton affinities. This seems surprising because Li^+ association is largely electrostatic[41] and the large polarizabilities associated with S and P bases should favor bonding to Li^+. Additional measurements would obviously be helpful.

Conclusions: $H(OH_2)_2^+$ can be produced at low pressure ($<10^{-5}$ torr) in the gas phase by a sequence of bimolecular reactions in mixtures of CH_3CHX_2 (X = F, Cl, Br) or $(CF_2H)_2O$ and H_2O. By adding small quantities of other Lewis bases to these mixtures, solvated proton transfer reactions can be studied. Observations of the preferred direction of H_3O^+ transfer between a series of bases containing heteroatoms of first and second row elements demonstrate that bases containing S or P heteroatoms bind H_3O^+ more weakly than O or N bases with comparable proton affinities. Viewing the hydrogen bond in $BH(OH_2)^+$ complexes as a composite of contributions from both $B\cdots HOH_2^+$ and $BH^+\cdots OH_2$ facilitates an understanding of this second row effect. It is mainly due to the decreased electronegativity of second row elements so that the partial charge on protons bound to S and P heteroatoms is minimal and stabilizing contributions from the $BH^+\cdots OH_2$ configuration is therefore weakened. Since bonding in $BH(OH_2)^+$ complexes is delocalized over three nuclear centers and involves four electrons, direct comparison of H_3O^+ affinities with Li^+

or H^+ affinities is not straightforward. However, lithium ion affinities also appear to exhibit weaker bonding to S containing bases than O or N bases with comparable proton affinities.

Acknowledgment: This research was supported in part by the Army Research Office.

References

(1) Fehsenfeld, F. C.; and Ferguson, E. E. J. Chem. Phys. 1973, 59, 6272.

(2) Fehsenfeld, F. C.; Dotan, I.; Albritton, D. I.; Howard, C. J.; and Ferguson, E. E., J. Geophys. Res. 1978, 83, 1333.

(3) Fehsenfeld, F. C.; Mosesman, M.; and Ferguson, E. E. J. Chem. Phys., 1971, 55, 2115.

(4) Hiraoka, K.; and Kebarle, P. J. Am. Chem. Soc. 1977, 99, 360.

(5) Olmstead, W. N.; Lev-On, M.; Golden, D. M.; and Brauman, J. I. J. Am. Chem. Soc. 1977, 99, 992.

(6) Jasinski, J. M.; Rosenfeld, R. N.; Golden, D. M.; and Brauman, J. I. J. Am. Chem. Soc. 1979, 101, 2259.

(7) Kambara, H.; and Kanomata, I. Int. J. Mass Spectrom. Ion Phys. 1977, 25, 129.

(8) Cates, R. D.; and Bowers, M. T. J. Am. Chem. Soc., 1980, 102, 3994.

(9) Bomse, D. S. and Beauchamp, J. L. J. Am. Chem. Soc., submitted.

(10) Smith, D.; Adams, N. G.; and Henchman, M. J. J. Chem. Phys. 1980, 72, 4951.

(11) Tanaka, K.; Mackay, G. I.; and Bohme, D. K. Can. J. Chem. 1978, 56, 193.

(12) Meot-Ner, M. J. Am. Chem. Soc. 1979, 101, 2389.

(13) Mackay, G. I.; Tanner, S. D.; Hopkinson, A. C.; and Bohme, D. K. Can. J. Chem. 1979, 57, 1516.

(14) Ridge, D. P.; and Beauchamp, J. L.; J. Am. Chem. Soc. 1974, 96, 637.

References (continued)

(15) Holtz, D.; Beauchamp, J. L.; and Woodgate, S. D. J. Am. Chem. Soc. 1970, 92, 7484.

(16) Speranza, M.; and Angelini, G. J. Am. Chem. Soc., in press.

(17) Angelini, G.; and Speranza, M. J. Am. Chem. Soc., in press.

(18) Huang, J. T. J.; and Schwartz, M. E. J. Chem. Phys. 1972, 56, 755.

(19) Meot-Ner, M.; and Field, F. H. J. Am. Chem. Soc. 1977, 99, 998.

(20) Desmueles, P. J.; and Allen, L. C. Chem. Rev. in press.

(21) Newton, M. D.; and Ehrenson, S. J. Am. Chem. Soc. 1971, 93, 4971.

(22) Merlet, P.; Peyerimhoff, S. D.; and Buenker, R. J. J. Am. Chem. Soc. 1972, 94, 8301.

(23) Newton, M. D. J. Chem. Phys. 1977, 67, 5535.

(24) Bomse, D. S.; and Beauchamp, J. L. J. Am. Chem. Soc., submitted for publication.

(25) Hiraoka, K.; Grimsrud, E. P.; and Kebarle, P. J. Am. Chem. Soc. 1974, 96, 3359.

(26) Meot-Ner, M. J. Am. Chem. Soc. 1978, 100, 4694.

(27) Kebarle, P. Annu. Rev. Phys. Chem. 1977, 28, 445.

(28) Bohme, D. K.; Mackay, G. I.; and Tanner, S. D. J. Am. Chem. Soc. 1979, 1 1, 3724.

(29) Hiraoka, K.; and Kebarle, P. Can. J. Chem. 1977, 55, 24.

(30) Cunningham, A. J.; Payzant, J. D.; and Kebarle, P. J. Am. Chem. Soc. 1972, 94, 7627.

References (continued)

(31) Lau, Y. K.; Saluja, P. P. S.; and Kebarle, P. J. Am. Chem. Soc., in press.

(32) Davidson, W. R.; Sunner, J.; and Kebarle, P. J. Am. Chem. Soc. 1979, 101, 1675.

(33) Berman, D. W.; and Beauchamp, J. L. J. Phys. Chem. 1980, 84, 2233.

(34) Price, P.; Martensen, D. P.; Upham, R. A.; Swofford, H. S. and Buttrill, S. E. Anal. Chem. 1975, 47, 190.

(35) Buttrill, S. E.; Reynolds, W. L.; and Knoll, K. A.; Inorg. Chem. 1976, 15, 2323.

(36) Martinsen, D. P.; and Buttrill, S. E., Org. Mass. Spectrom. 1976, 11, 762.

(37) Martinsen, D. P.; and Buttrill, S. E. J. Am. Chem. Soc. 1978, 100, 6559.

(38) See for example: Bartmes, J. E.; Scott, J. A.; and McIver, R. T. J. Am. Chem. Soc. 1979, 101, 6046.

(39) See for example: Wolf, J. F.; Staley, R. H.; Koppel, I.; Taagepera, M.; McIver, R. T.; Beauchamp, J. L.; and Taft, R. W. J. Am. Chem. Soc. 1977, 99, 5417.

(40) Clair, R. L.; and McMahan, T. Can. J. Chem. 1980, 58, 863.

(41) Woodin, R. L.; and Beauchamp, J. L. J. Am. Chem. Soc. 1978, 100, 501.

(42) Beauchamp, J. L. Annu. Rev. Phys. Chem. 1971, 22, 527.

(43) Beauchamp, J. L.; Holtz, D.; Woodgate, S. D.; and Patt, S. L. J. Am. Chem. Soc. 1972, 94, 2798.

References (continued)

(44) McMahan, T. B.; and Beauchamp, J. L. Rev. Sci. Instrum. 1972, 43, 509.

(45) Berman, D. W.; Anicich, V.; and Beauchamp, J. L. J. Am. Chem. Soc. 1979, 101, 1239.

(46) It should be noted that the mass degeneracy of $CH_3CF_2^+$ and $CH_3CHF(OH_2)^+$ was a minor complication impeding certain double resonance experiments in these mixtures. Based on data in Fig. 1, the calculated concentration of $CH_3CF_2^+$ was subtracted from the total ion signal at mass 65 amu to yield the net concentration of $CH_3CHF(OH_2)^+$ plotted in Fig. 2.

(47) As in earlier dihaloethane studies (see refs. 33, 45) mixtures of CH_3CHF_2 and H_2O were examined for the occurrence of two additional processes. Based on thermochemical data discussed in these other studies, the process

$$H_3O^+ + CH_3CHF_2 \rightarrow CH_3CHF^+ + HF + H_2O$$

is expected to be endothermic. CH_3CHF^+ exhibits a positive double resonance signal from H_3O^+ in agreement with this expectation. Again mimicking the earlier dihaloethane studies, the exothermic reaction $CH_3CHF^+ + H_2O \rightarrow CH_3CHOH^+ + HF$ is not observed.

(48) Lindemann, E.; Rozett, R. W.; and Koski, W. S. J. Chem. Phys. 1972, 56, 5490.

(49) Cotten, R. J.; and Koski, W. S. J. Chem. Phys. 1973, 59, 784.

(50) Berman, D. W.; and Beauchamp, J. L. J. Am. Chem. Soc., to be submitted.

References (continued)

(51) Bensen, S. W. "Thermochemical Kinetics: Methods for the Estimation of Thermochemical Data and Rate Parametrics", 2nd Ed., Wiley, New York, 1976.

(52) Beauchamp, J. L.; and Caserio, M. J. J. Am. Chem. Soc., 1972, 94, 2638.

(53) Beauchamp, J. L.; Holtz, D.; Woodgate, S. D.; and Patt, S. L. J. Am. Chem. Soc. 1972, 94, 2798.

(53) Pauling, L. "The Nature of the Chemical Bond", 3rd ed.; Cornell University Press, Ithaca, 1960, pp. 97-102.

(54) The observed tendency of oxygen containing bases to form proton bond dimers and other clusters excluding H_2O, Table II, demonstrates that such bases will bond as readily to each other as to water and suggests that hydrogen bond strengths in these clusters are not a strong function of the choice of oxygen bases involved in each cluster.

CHAPTER III

REACTIONS OF DISOLVATED PROTONS. COMPETITION BETWEEN H^+ AND H_3O^+ TRANSFER TO BASES OF VARYING STRENGTHS

Reactions of Disolvated Protons. Competition Between H^+ and H_3O^+ Transfer to Bases of Varying Strengths

D. W. Berman and J. L. Beauchamp

Contribution No. from the Arthur Amos Noyes Laboratory of Chemical Physics, California Institute of Technology, Pasadena, California 91125. (Received)

Abstract

The relative importance of H_3O^+ transfer and H^+ transfer from $H(OH_2)_2^+$ to a series of Lewis bases is observed to be a function of base strength. H^+ transfer is first observed with CH_3COOH (PA = 191.7 kcal mol^{-1}) and increases in importance with increasing proton affinity of the base until at PA(B) = 206 kcal mol^{-1}. NH_4^+ is the sole product of encounters between NH_3 and $H(OH_2)_2^+$ so that H_3O^+ transfer is no longer observed. The nature of neutral products formed during H^+ transfer is also considered.

I. Introduction

Recent investigations in our laboratory[1,2] and elsewhere[3] have revealed bimolecular reaction sequences which lead to formation of the disolvated proton, $H(OH_2)_2^+$, at low pressures ($<10^{-5}$ torr). These findings make it possible to study the chemistry of this interesting and important entity using the techniques of ion cyclotron resonance spectroscopy. Though proton bound clusters are generally observed at higher pressures ($>10^{-1}$ torr) as products of termolecular association reactions,[4] eq. 1, such processes are unimportant at reduced particle

$$BH^+ + B \rightleftharpoons [BHB^+]^* \xrightarrow{[M]} BHB^+ \qquad (1)$$

densities. However, the proton bound dimer of water is produced via a sequence of bimolecular reactions following electron impact ionization in two component mixtures containing H_2O and either CH_3CHX_2 (X = F, Cl, Br)[1,2] or $(CF_2H)_2O$.[3] $H(OH_2)_2^+$ is unreactive in these mixtures. When small quantities of various Lewis bases are added to the system, however, two reactions are observed. These are H_3O^+ transfer, eq. 2, and proton transfer, eq. 3. In the proton transfer reaction there are two possibilities for the neutral products, where either two molecules of H_2O or the stable dimer may be formed, eqs. 3 and 4, respectively.

$$H(OH_2)_2^+ + B \longrightarrow \begin{cases} BH(OH_2)^+ + H_2O & (2) \\ BH^+ + 2H_2O & (3) \\ BH^+ + (H_2O)_2 & (4) \end{cases}$$

A series of mixtures were examined in this study to assess factors affecting the competition between H_3O^+ transfer and H^+ transfer from $H(OH_2)_2^+$ to n-donor bases. The relative importance of reactions 3 and 4 are also considered.

II. Experimental

Ion cyclotron resonance instrumentation and techniques have been previously described in detail.[5-7] Experiments were carried out at ambient temperature (25° C). Neutral pressures ranged between 1.0×10^{-8} - 1.0×10^{-5} torr. Pressures were measured on a Schulz-Phelps type ionization gauge calibrated against an MKS Baratron Model 90H1-E capacitance manometer. Pressures measured by this technique should be accurate to ± 20%. Except as noted, chemicals used in this work were obtained from commercial sources. HCN was generated from KCN and acid, and distilled under vacuum. Formaldehyde was prepared fresh before each experiment from thermal decomposition of paraformaldehyde. All samples were degassed by several freeze-pump-thaw cycles to remove noncondensable contaminants.

III. Results

Formation of the doubly solvated proton, $H(OH_2)_2^+$. The mechanism of formation of $H(OH_2)_2^+$ at low pressures has been described in detail.[1-3] Briefly, in mixtures containing H_2O and one of the dihaloethanes CH_3CHX_2 (X = F, Cl, Br),[1,2] H_3O^+ reacts with CH_3CHX_2 to yield a bifunctional intermediate $CH_3CHXOH_2^+$, eq. 5. Though in some cases $CH_3CHXOH_2^+$ retains sufficient internal energy to eliminate a second

molecule of HX, eq. 6, the majority reacts with H_2O yielding the proton bound dimer of water, eq. 7.

$$H_3O^+ + CH_3CHX_2 \xrightarrow{60\%} CH_3CHXOH_2^+ + HX \quad (5)$$

$$H_3O^+ + CH_3CHX_2 \xrightarrow{40\%} CH_3CHOH^+ + 2\,HX \quad (6)$$

$$CH_3CHXOH_2^+ + H_2O \rightarrow H(OH_2)_2^+ + CH_2CHX \quad (7)$$

When $(CF_2H)_2O$ is mixed with H_2O,[3] two sequences of reactions are observed. Both ultimately yield $H(OH_2)_2^+$. One of two major species present at short time, CF_2H^+, abstracts a fluorine from $(CF_2H)_2O$ yielding CF_2HOCFH^+, eq. 8. CF_2HOCFH^+ then reacts sequentially with

$$CF_2H^+ + (CF_2H)_2O \rightarrow CF_2HOCFH^+ + CF_3H \quad (8)$$

two molecules of H_2O, eqs. 9 and 10, producing $H(OH_2)_2^+$. In the second

$$CF_2HOCFH^+ + H_2O \rightarrow CF_2HOH_2^+ + HCFO \quad (9)$$

$$CF_2HOH_2^+ + H_2O \rightarrow H(OH_2)_2^+ + CF_2 \quad (10)$$

sequence, H_3O^+ reacts with $(CF_2H)_2O$ to yield the proton bound dimer $HCFOHOH_2^+$, eq. 11. $H(OH_2)_2^+$ is produced from this species by transfer of a hydrated proton, eq. 12.

$$H_3O^+ + (CF_2H)_2O \rightarrow HCFOHOH_2^+ + CF_3H \quad (11)$$

$$HCFOHOH_2^+ + H_2O \rightarrow H(OH_2)_2^+ + HCFO\,. \quad (12)$$

In the present studies, several of these mixtures were employed in specific instances so that mass degeneracies between ions involved in the production of $H(OH_2)_2^+$ and the other ions of interest in these studies could be avoided.

Reactions of $H(OH_2)_2^+$ with n-donor bases: Dimethyl ether as an example. When small quantities of n-donor bases are added to one of the mixtures capable of yielding the proton bound dimer of water, several reactions between $H(OH_2)_2^+$ and the added base are observed. To illustrate the type of chemistry that occurs in such mixtures, trapped ion data obtained in a 6.8:48:1 mixture of $(CF_2H)_2O$, H_2O and $(CH_3)_2O$ are presented in Fig. 1. The complicated chemistry involved in the production of $H(OH_2)_2^+$ dominates for the first 400 msec and has been omitted for clarity. Species present after 400 msec include $H(OH_2)_2^+$, $(CH_3)_2OH^+$, $(CH_3)_2OH(OH_2)^+$, and $[(CH_3)_2O]_2H^+$. These are the only ions depicted in Fig. 1. The concentrations of all other ions are negligible after 400 msec and are not included in the normalization. Encounters between $H(OH_2)_2^+$ and $(CH_3)_2O$ result in hydrated proton transfer, eq. 13. Double resonance experiments confirm that in a small number of cases protonated dimethyl ether is the observed product. This is represented by both eqs. 14 and 15 to indicate uncertainty in the nature of neutral products. It should be noted, however, that proton transfer from H_3O^+ at short times, eq. 16, is the major source of $(CH_3)_2OH^+$ in this system. Contributions from processes 14 and 15 to the total intensity of $(CH_3)_2OH^+$ are determined as follows. The temporal variation of $(CH_3)_2OH^+$ abundance was monitored twice, once

FIGURE 1. Variation of ion abundance with time following a 20 msec, 70.0 eV electron beam pulse in a 1:6.8:48 mixture of $(CH_3)_2O$, $(CF_2H)_2O$ and H_2O at a total pressure of 1.7×10^{-6} torr. Ions involved in the initial production of $H(OH_2)_2^+$ are omitted for clarity. Concentrations of these species are negligible after 400 msec and are not included in the normalization.

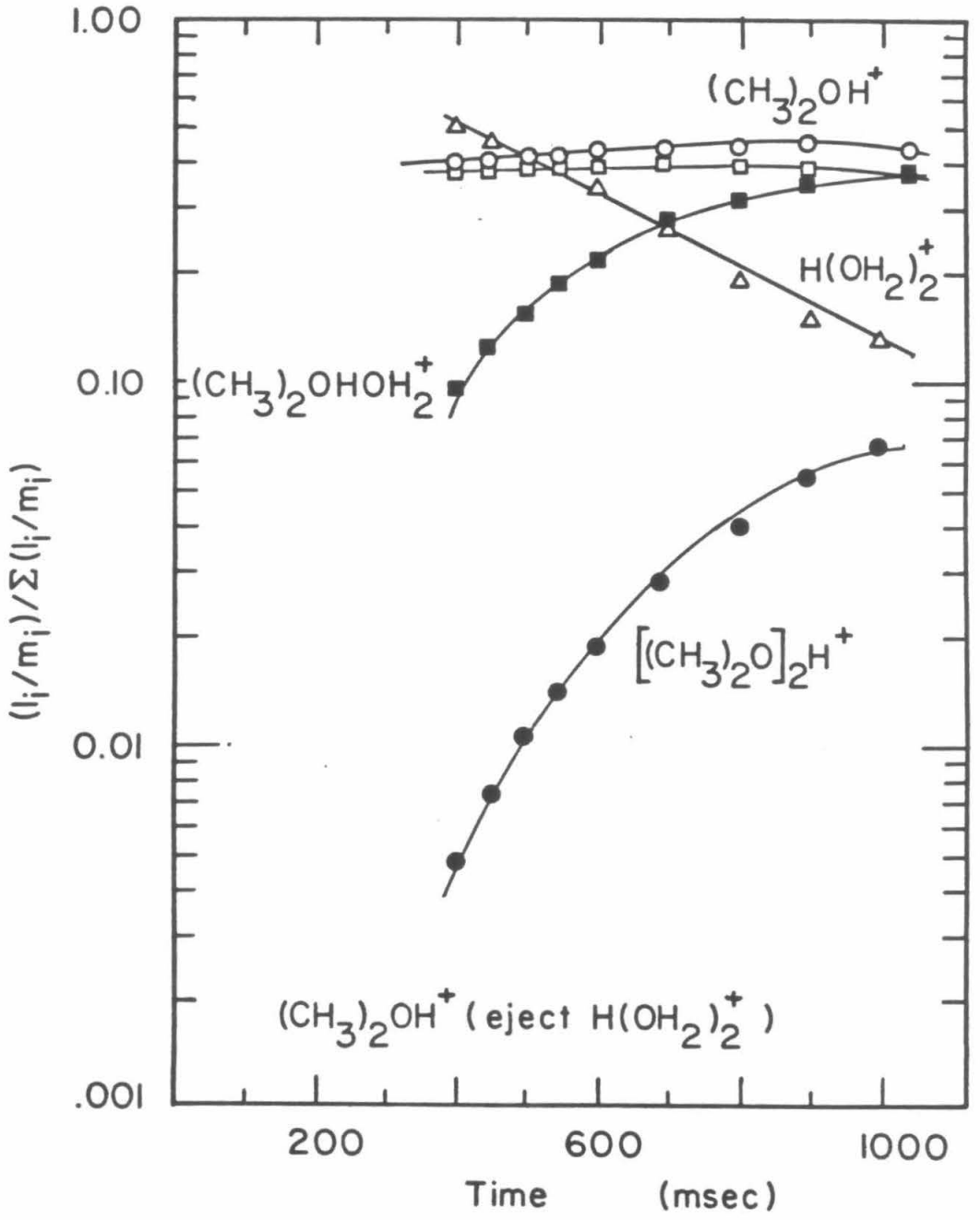
1.00
0.10
0.01
.001
$(I_i/m_i)/\Sigma(I_i/m_i)$
$(CH_3)_2OH^+$
$H(OH_2)_2^+$
$(CH_3)_2OHOH_2^+$
$[(CH_3)_2O]_2H^+$
$(CH_3)_2OH^+$ (eject $H(OH_2)_2^+$)
200
600
1000
Time (msec)

$$H(OH_2)_2^+ + (CH_3)_2O \xrightarrow{85\%} (CH_3)_2OH(OH_2)^+ + H_2O \quad (13)$$

$$H(OH_2)_2^+ + (CH_3)_2O \xrightarrow{15\%} (CH_3)_2OH^+ + 2H_2O \quad (14)$$

$$H(OH_2)_2^+ + (CH_3)_2O \xrightarrow{15\%} (CH_3)_2OH^+ + (H_2O)_2 \quad (15)$$

$$H_3O^+ + (CH_3)_2O \rightarrow (CH_3)_2OH^+ + H_2O \quad (16)$$

while $H(OH_2)_2^+$ was being continually ejected from the system with a tuned rf signal and a second time in the absence of any double resonance ejection. The difference in $(CH_3)_2OH^+$ intensities monitored under these two conditions represents $(CH_3)_2OH^+$ produced specifically from $H(OH_2)_2^+$, eqs. 14 and 15. Both curves are presented in Fig. 2.

The proton bound dimer of dimethyl ether is also produced in this system, eq. 17. Processes involving $H(OH_2)_2^+$, eqs. 13-15, have already

$$(CH_3)_2OHOH_2^+ + (CH_3)_2O \rightarrow [(CH_3)_2O]_2H^+ + H_2O \quad (17)$$

been generalized in eqs. 2-4, respectively. Reaction 17 is an example of the generalized exchange process 18.

$$BH(OH_2)^+ + B \rightarrow HB_2^+ + H_2O \quad (18)$$

Summary of observed reactions of $H(OH_2)_2^+$ with n-donor bases.

Reactions between $H(OH_2)_2^+$ and other n-donor bases in the various three-component mixtures surveyed, are entirely represented by the generalized processes 2-4. Table I presents results for 25 bases studied in this and related work. Proton affinities are also given for each base listed.[8]

FIGURE 2. Variation of $(CH_3)_2OH^+$ with time in a 1:6.8:48 mixture of $(CH_3)_2O$, $(CF_2H)_2O$, and H_2O at a total pressure of 1.7×10^{-6} torr. The upper plot represents the total abundance of $(CH_3)_2OH^+$ while the lower plot is obtained while continually ejecting $H(OH_2)_2^+$ from the cell so that contributions from this ion to the abundance of $(CH_3)_2OH^+$ are removed.

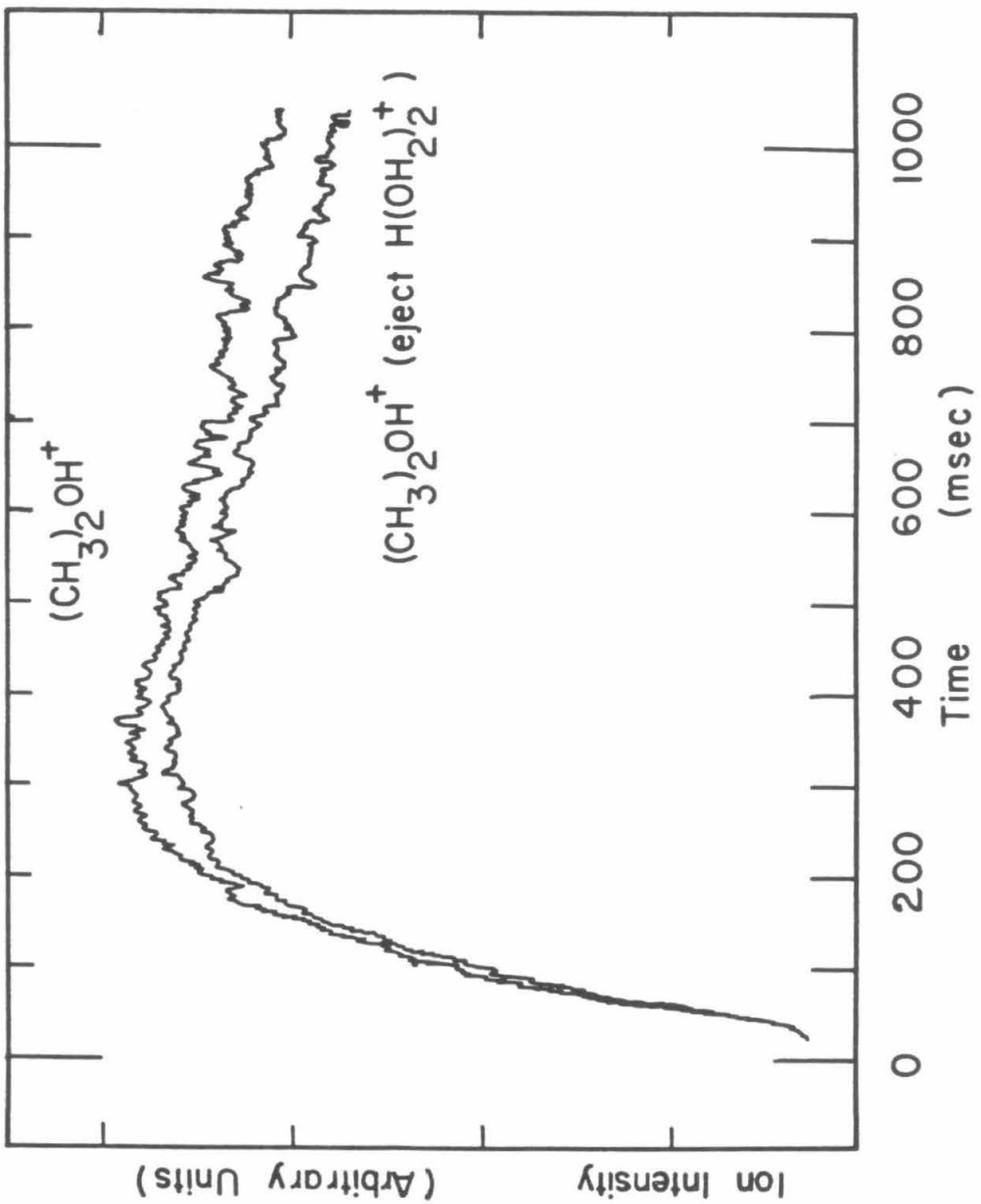
Ion Intensity
(Arbitrary Units)
0
200
400
600
800
1000
Time (msec)
$(CH_3)_2OH^+$
$(CH_3)_2OH^+$ (eject $H(OH_2)_2^+$)

Table I. Measured Rate Constants for Hydrated Proton Transfer and Proton Transfer

	Species	PA[a]	k_{Total}[b]	k_A[c]	k_B[d]	% proton transfer
	H_2O	174				
1	H_2S	177.6	<0.001[e]	<0.001[e]	0	0
2	HCN	178.2	15.5 1.0[e]	15.5	0	0
3	H_2CO	178.3	18.0 30 ± 20[f]	18.0	0	0
4	CF_2HCH_2OH	181.6	17.7	17.7	0	0
5	HCOOH	183.8	17.3 24 ± 7[f]	17.3	0	0
6	C_6H_6	185.1	not observed	0	0	0
7	CH_3OH	185.9	20.5 24 ± 6[f]	20.5	0	0
8	CH_3CHO	188.7	15.0 31 ± 8[f]	15.0	0	0
9	CH_3SH	189.6	18.9	18.9	0	0
10	CH_3CH_2OH	190.4	25 ± 6[f]	25 ± 6[f]	0[f]	0

Table I. Continued

	Species	PA	k_{total}	k_A	k_B	% proton transfer
11	PH_3	191.1	13.1	13.1	0	0%
12	CH_3COOH	191.7	13.5	12.1	1.35	10%
			27 ± 8[f]			
13	$C_6H_5CH_3$	192.4	4.6	0	4.59	100%
14	$CH_3CH_2CH_2CHO$	193.4	20.6	15.7	4.94	24%
15	$(CH_3)_2O$	193.8	21.9	18.6	3.30	15%
			22 ± 6[f]			
16	o-$C_6H_4(CH_3)_2$	194.8	16.8	0	16.8	100%
17	p-dioxane	195.0	19.1	13.2	5.9	31%
18	$(CH_3)_2CO$	197.6	25.5	12.7	12.7	50%
			35 ± 9[f]			
19	tetrahydrofuran	200.1	25.0	2.5	22.5	90%
20	$(CH_3)_2S$	201.3	24.1	<0.01	(24.1 ± 8)	>99%
21	$(CH_3CH_2)_2O$	201.7	19.5	0.98	18.5	95%
22	$(CH_3)_3CCO(CH_3)$	203.3	24.0	0.48	23.6	98%
23	CH_3PH_2	205.5	17.3	<0.01	(17.3 ± 8)	>99%
24	NH_3	206	33.8	not observed	33.8	100%
			26[g]			
25	CH_3NH_2	215		not observed		100%

[a]Units are kcal mol^{-1}. Values are from Ref. 8.

[b]Units are 10^{-10} cm^3 $molecule^{-1}$ sec^{-1}. Values measured in this study should be accurate within 20% except as noted.

Table I. Footnotes continued

---

[c]Units are 10^{-10} cm^3 $molecule^{-1}$ sec^{-1}. Subscript A refers to hydrated proton transfer: $H(OH_2)_2^+ + B \rightarrow BH(OH_2)^+ + H_2O$

[d]Units are 10^{-10} cm^3 $molecule^{-1}$ sec^{-1}. Subscript B refers to proton transfer: $H(OH_2)_2^+ + B \rightarrow BH^+ + (2H_2O)$. The neutral product is either the stable water dimer or 2 molecules of H_2O, see text.

[e]K. Tanaka, G. I. Mackay, and D. K. Bohme, Can. J. Chem., 56, 193 (1978).

[f]D. K. Bohme, G. I. Mackay, and S. D. Tanner, J. Am. Chem. Soc. 101, 3724 (1979).

[g]F. C. Fehsenfeld and E. E. Ferguson, J. Chem. Phys. 59, 6272 (1973).

IV. Discussion

The relative importance of hydrated proton transfer, eq. 2, and proton transfer, eqs. 3 and 4, from $H(OH_2)_2^+$ is a strong function of the acceptor base strength as evident in Fig. 3 where the fraction of reactive encounters that proceed by proton transfer is plotted as a function of the proton affinity of B. In Fig. 3, proton transfer is not observed until the proton affinity of B reaches 192 kcal $mole^{-1}$. Then encounters yielding BH^+ increase in importance relative to production of $BH(OH_2)^+$ with increasing proton affinity of the Lewis bases in each mixture. When basicity of these species reach 206 kcal $mole^{-1}$, $BH(OH_2)^+$ production essentially ceases and processes 3 and 4 account for 100% of the yield from reactions between $H(OH_2)_2^+$ and B. The behavior depicted in Fig. 3 can be understood in terms of the energetics associated with these processes.

Energetics of reactions observed in these mixtures are illustrated in Fig. 4. $(CH_3)_2O$ is used as an example because all of the required thermochemistry for this system is available in the literature.[8-10] General relationships presented in the center of this figure, however, are applicable to any of the systems studied. Thus enthalpies of reaction for processes 2, 3 and 4 can be determined from the following relationships, eqs. 19, 20 and 21. The proton affinity of the neutral water dimer can also be obtained from this figure, eq. 22. From $D(H_2O\text{-}H_3O^+)$ = 32 kcal mol^{-1},[9] $D(H_2O\text{-}H_2O)$ = 5.0 kcal mol^{-1},[11] and employing thermochemical quantities listed in Table I, the minimum acceptor base strength for which processes 3 and 4 each become exo-

FIGURE 3. Relationship between the extent of H^+ transfer and proton affinities of the acceptor base B. % H^+ transfer represents the fraction of BH^+ produced from encounters between $H(OH_2)_2^+$ and B compared to the total product concentration, $BH^+ + BH(OH_2)^+$. This is plotted as a function of PA(B) on the bottom of the figure or PA(B) - $PA(H_2O)$ on the top of the figure, see text. Numbers correspond to bases listed in Table I.

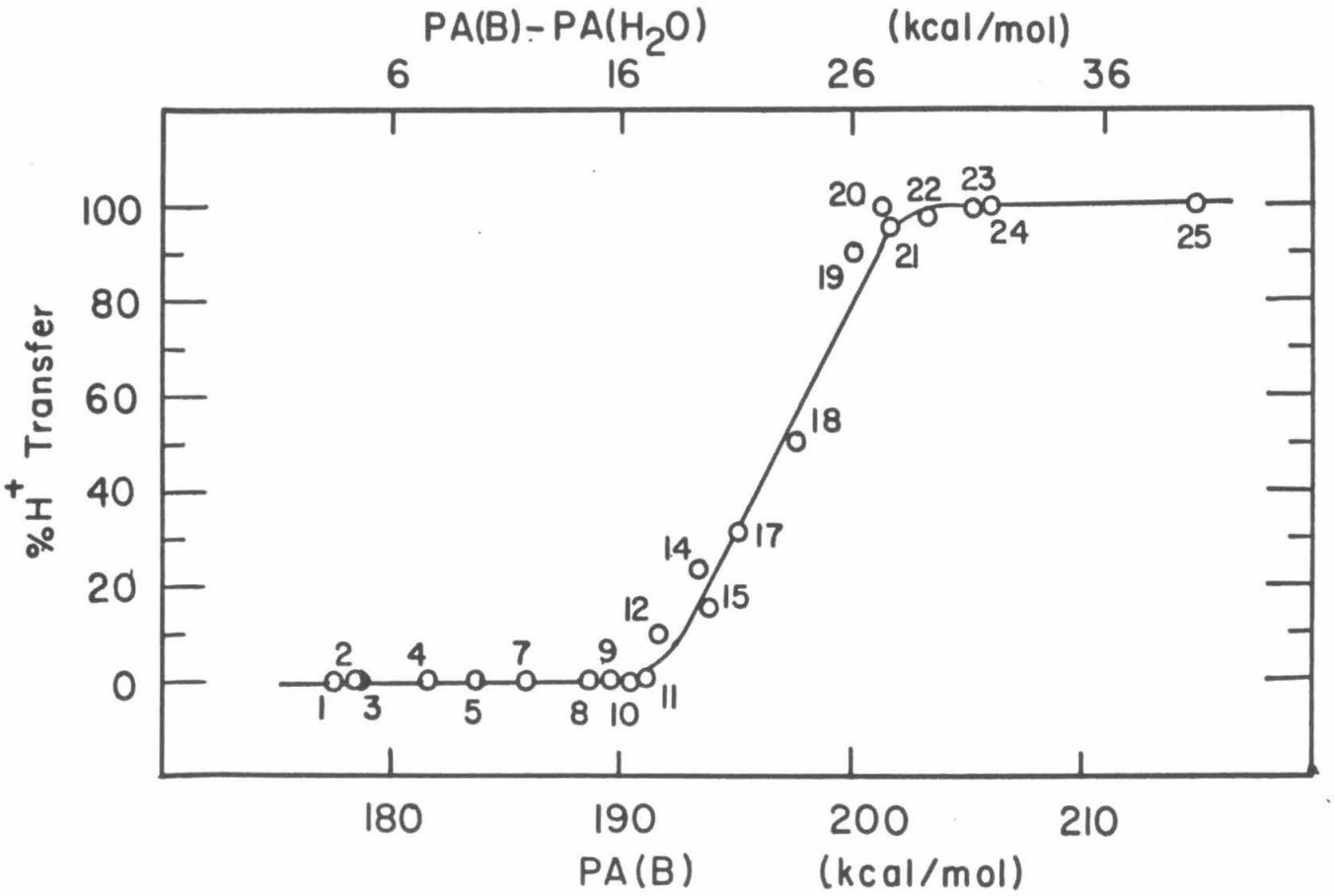
PA(B)-PA(H2O) (kcal/mol)
6
16
26
36
100
80
60
40
20
0
%H+ Transfer
1
2
3
4
5
7
8
9
10
11
12
14
15
17
18
19
20
21
22
23
24
25
180
190
200
210
PA(B) (kcal/mol)

FIGURE 4. Energetics of reactants, products, and intermediates for reactions ocurring between $H(OH_2)_2^+$ and $(CH_3)_2O$. Values are derived from thermochemical data found in refs. 8 and 9. General relationships between reaction enthalpies of these processes and proton affinities, H_3O^+ affinities, and H_2O^+affinities of the species involved are depicted as well.

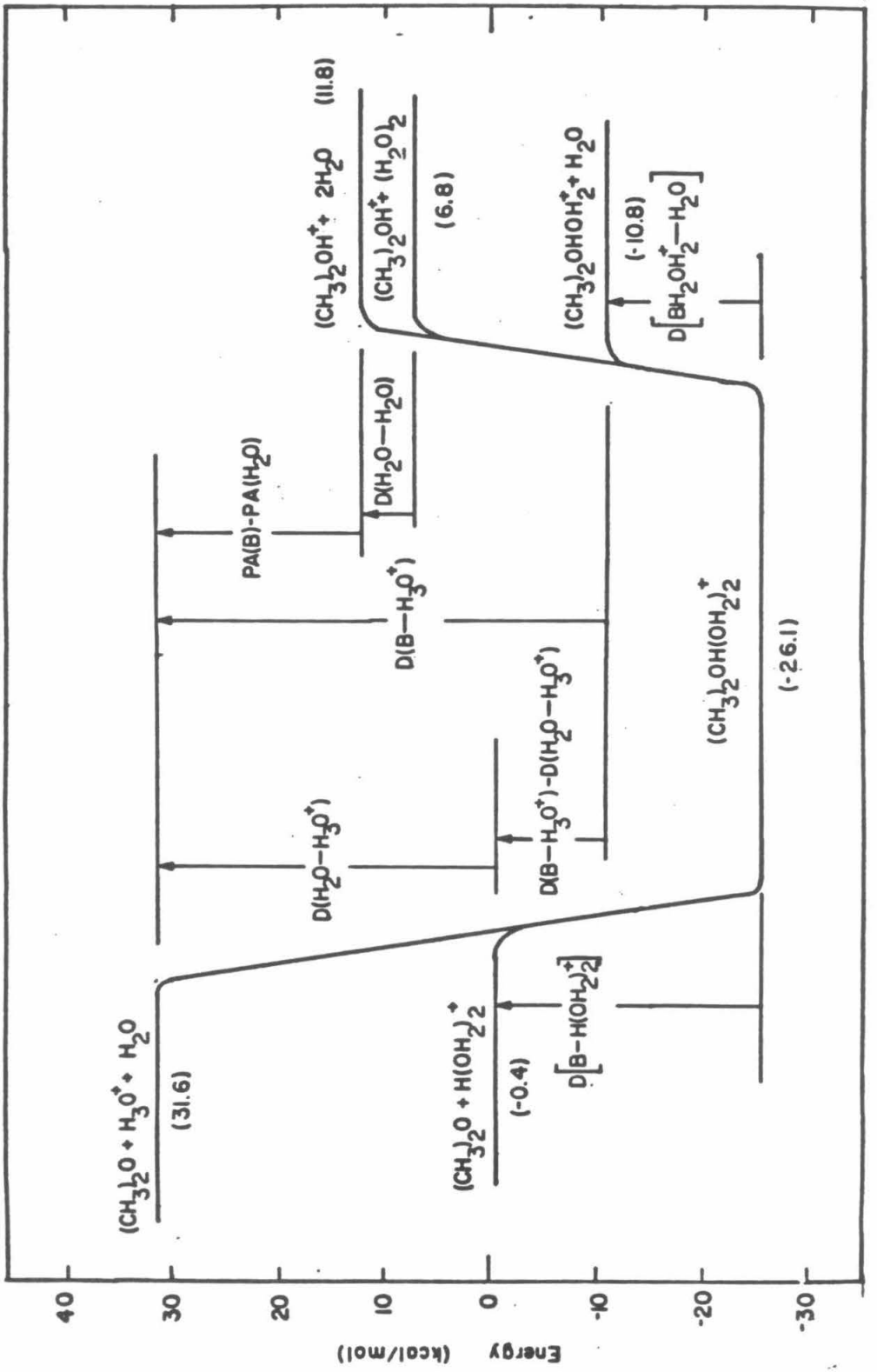
Energy (kcal/mol)
40
30
20
10
0
-10
-20
-30
(CH3)2O + H3O+ + H2O
(31.6)
(CH3)2O + H(OH2)2+
(-0.4)
D[B-H(OH2)2+]
D(H2O-H3O+)
PA(B)-PA(H2O)
D(B-H3O+)
D(B-H3O+)-D(H2O-H3O+)
(CH3)2OH(OH2)2+
(-26.1)
(CH3)2OH+ 2H2O (11.8)
(CH3)2OH+ (H2O)2
(6.8)
D(H2O-H2O)
(CH3)2OHOH2+ H2O
(-10.8)
D[BH2OH2+-H2O]

$$\Delta H_2 = -[D(B\text{-}H_3O^+) - D(H_2O\text{-}H_3O^+)] \quad (19)$$

$$\Delta H_3 = D(H_2O\text{-}H_3O^+) + [PA(H_2O)\text{-}PA(B)] \quad (20)$$

$$\Delta H_4 = \Delta H_3 - D(H_2O\text{-}H_2O) \quad (21)$$

$$PA[(H_2O)_2] = PA(B) + \Delta H_4 \quad (22)$$

thermic can be derived. Thus production of BH^+ from encounters between $H(OH_2)_2^+$ and B should be observed from process 4 only for bases with proton affinities $\geq$ 201 kcal mol^{-1}. Process 3 should not begin to contribute until PA(B) reaches at least 206 kcal $mole^{-1}$. Yet, $CH_3COOH_2^+$ is produced in a small number of encounters between $H(OH_2)_2^+$ and CH_3COOH (PA = 191.7 kcal mol^{-1}). In fact, 50% of the products from reaction between $H(OH_2)_2^+$ and $(CH_3)_2CO$ (PA = 197.6 kcal mol^{-1}) is $(CH_3)_2COH^+$. There are several plausible explanations that can account for the apparent disparity between calculated and observed thresholds for production of BH^+. For example, uncertainty in the published thermochemical data employed in this paper could be a factor, so that a brief review of these values is in order.

First, proton affinities appear in eqs. 20 and 21 only as a difference relative to H_2O so that changes in the absolute values for these numbers would not affect the above conclusions as long as the relative spacing of basicities remains constant. Thus eq. 4 will be exothermic for any base with a proton affinity at least 27 kcal mol^{-1} greater than H_2O. Scales of relative proton affinities for a large number of bases have been determined from measurements of proton transfer

equilibria employing the techniques of ICR,[8,12] and high pressure mass spectrometry.[13] Values from such equilibria are expected to be accurate within ± 0.2 kcal mol^{-1}. Errors will be compounded, however, as the number of steps required to link different bases increases. For species of interest in this study, proton affinities lie between H_2O and NH_3. Two different ICR studies yield $PA(NH_3)$-$PA(H_2O)$ = 32.0 kcal mol^{-1} at 300° K.[8,12] When the high pressure studies are corrected for temperature effects, this same proton affinity spread is found to be 32.0 kcal mol^{-1}.[9,13] Thus an uncertainty no greater than ± 1 kcal mol^{-1} would be a reasonable estimate for relative proton affinities presented in this paper. It should be noted that independent absolute proton affinity measurements for $PA(NH_3)$ and $PA(H_2O)$ do not always differ by 32 kcal mol^{-1}.[14] Of these techniques, however, only photoionization experiments are sufficiently precise to consider here. Since equilibria measurements represent true thermodynamic quantities and threshold measurements represent state to state transitions, direct comparisons between these techniques must be considered carefully. $D(NH_3\text{-}H^+)$ = 202.1 ± 1.3 kcal mol^{-1} has been obtained from photoionization of Van der Waals dimers of NH_3[15] employing a series of thermochemical cycles which include a 3.5 kcal mol^{-1} bond energy for the neutral dimer.[16] This represents a 0° K measurement. Similarly, $D(H_2O\text{-}H^+)$ = 165.8 ± 1.8 kcal mol^{-1} at 0° K.[17] Using 5.5 ± 0.5 kcal mol^{-1} for the 0° K bond energy of the neutral water dimer,[10] $D(H_2O\text{-}H^+)$ can be updated to 167.4 ± 1.8 kcal mol^{-1}. From these two absolute determinations, $PA(NH_3)$ - $PA(H_2O)$ = 34.7 ± 2 kcal mol^{-1} is determined for 0° K. At 298° K this values becomes ΔPA = 32.5 ± 2 kcal mol^{-1} in excellent agreement

with relative proton affinity determinations. A summary of these determinations is presented in Table II.

Measurements of the neutral water dimer bond energy and the enthalpy of association for the proton bound dimer of water are also summarized in Table II. The enthalpy of association for proton bound dimers of water has been determined from the temperature dependence of equilibrium constants for reaction 23.[4,18,19] As apparent in Table II, these studies are in agreement. The best estimate for the enthalpy

$$H_3O + H_2O \rightleftharpoons H(OH_2)_2^+ \qquad (23)$$

change of reaction 23 at 298° K is 32 ± 2 kcal mol^{-1}.[9] Recent theoretical and experimental determinations of $D(H_2O\text{-}H_2O)$ coincide closely when internal energy contributions and temperature effects are accounted for.[10,20,21] Thus the best estimate for this value seems to be 5.0 ± 1 kcal mol^{-1} at 298° K.[11] Summing uncertainty contributions from these three sets of data, calculated thresholds in eqs. 20 and 21 should be precise to ± 5 kcal mol. Assuming a 5 kcal mol^{-1} error, production of BH^+ would first occur when $PA(B) - PA(H_2O)$ = 22 kcal mol^{-1}. As depicted in Fig. 3, however, the product BH^+ is observed when $PA(B) - PA(H_2O)$ = 18 kcal mol^{-1}. It is thus unlikely that systematic errors of this type are entirely responsible for the 10 kcal mol^{-1} gap between the calculated and observed threshold for BH^+ production.

Another plausible explanation would be to assume that at threshold the thermal internal energy content of the reactants, $H(OH_2)_2^+$ and B, can contribute to the energy of reaction leaving cold products. It is reasonable to expect that a majority of the internal modes of a molecule

Table II. A Survey of Thermochemical Quantities Associated with the Energetics of Proton Transfer.[a]

$PA(H_2O)$[b]	$PA(NH_3)$[b]	ΔPA[b]	temperature[c]	ΔPA_{298}[d]	technique
		32.0[e]	298° K	32.0	ICR
		32.0[f]	298° K	32.0	ICR
		33.0[g]	600° K	32.0	High pressure mass spec
167.4 ± 1.8[h]	202.1 ± 1.3[j]	34.7	0° K	32.5	photoionization
			Best estimate:	32.0 ± 1	

$D(H_2O - H_3O^+)$

$-\Delta H$[k]	technique
33.0[l]	High Pressure Mass Spec
36.0[m]	High Pressure Mass Spec
31.6[n]	High Pressure Mass Spec
32.0 ± 2[o]	

$D(H_2O - H_2O)$

$-\Delta H$[p]	temperature[c]	$-\Delta H_{298}$	technique
3.63[q]	373° K	5.0	thermal conductivity
5.6[r]	0° K	5.1	calculation
6.1[s]	0° K	5.6	calculation
5.3[t]	0° K	4.8	calculation
	Best estimate:	5.0 ± 1	

Table II. (Continued)

---

[a]A general review of proton affinities can be found in Ref. 14. Results directly obtained from each study are referenced. All other entries in each row of the Table are derived from the referenced value.

[b]Units are kcal mol^{-1}.

[c]Entries in this column represent temperatures for which referenced results are appropriate.

[d]Units are kcal mol^{-1}. Values in this column were derived from referenced results using standard enthalpy tabulations from Ref. 24.

[e]Ref. 8.

[f]Ref. 12.

[g]Ref. 13.

[h]Ref. 17. The value cited in Ref. 17, 165.8 kcal mol^{-1} was reinterpreted employing $D(H_2O - H_2O)_{298} = 5.0$ kcal mol^{-1} from Ref. 10.

[j]Ref. 15.

[k]Units are kcal mol^{-1}. This represents the enthalpy charge for the process: $H_3O^+ + H_2O \rightarrow H(OH_2)_2^+$.

[l]Ref. 19.

[m]Ref. 18.

[n]Ref. 4.

[o]Ref. 9.

[p]Units are kcal mol^{-1}. This represents the enthalpy charge for the process: $H_2O + H_2O \rightarrow (H_2O)_2$.

[q]Ref. 10.

[r]Matsuka, O.; Clementi, E.; and Yashimine, M. J. Chem. Phys. 1896, 61, 1351.

Table II. (Continued)

---

[s]Diercksen, G. H. F.; Krasner, W. P.; and Roos, B. O. Theoret. Chim. Acta, 1875, 36, 249.

[t]Ref. 21.

(or ion) are coupled so that energy is rapidly and continually redistributed. There is a finite probability that the total internal energy of such a species will concentrate in a mode representing the reaction coordinate and therefore contribute to the energy of reaction.[22]

The average internal energy of a molecule or ion at 298° K can be derived from standard enthalpy functions, eq. 24.[23] Based on tabulations

$$(H^{\circ}_{298} - H^{\circ}_{0}) = E_{int} + 4RT \qquad (24)$$

of such functions[24] for species similar to those of interest in this study, the two reactants $H(OH_2)_2^+$ and B may each contain approximately 2 kcal mol^{-1} of internal energy. Assuming all of this energy is available for reaction, the average energy contribution from both reactants would be expected to lower the observed threshold for BH^+ formation by 4 kcal mol^{-1}. This represents less than half of the 10 kcal mol^{-1} required to account for behavior depicted in Fig. 3. However, molecules and ions in these experiments are not monoenergetic but exhibit a thermal distribution of energies and though the average energy of the reactants is too small to account for observed behavior, approximately 10% of these species in any of the mixtures can be expected to contain sufficient internal energy to permit BH^+ production for bases with proton affinities as low as observed. It therefore seems reasonable that thermal energy contributions can account for the production of BH^+ in reactions between $H(OH_2)_2^+$ and bases with proton affinities as low as 192 kcal mol^{-1} as observed. A more sophisticated treatment[22] of this problem would be necessary to confirm this hypothesis, however.

General features of the curve displayed in Fig. 3 can be understood in terms of the probable mechanism of reaction associated with processes 2-4. Reactions between $H(OH_2)_2^+$ and B most likely proceed through a long-lived complex, $BH(OH_2)_2^+$, which contains two hydrogen bonds linking the various base units, Structure I.[25] From this complex,

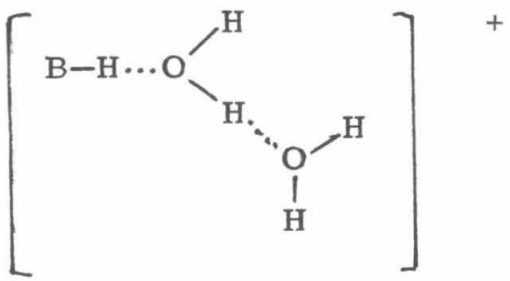

I

reactions 2, 3 and 4 all proceed by breaking of a similar type of hydrogen bond. Since electrons do not need to be recoupled when hydrogen bonds are broken, no appreciable activation barriers are expected from any of these processes. Thus assuming sufficient energy is available in the complex, the relative importance of reactions 2, 3 and 4 will be determined by statistical factors in the exit channels.[22] Statistical weights for the processes 2 and 4 should be roughly equivalent because each reaction involves the breaking of a single hydrogen bond yielding a pair of similar products, (a small neutral base and a proton bound dimer). Therefore, at energies sufficiently above threshold, the relative yield from reactions 2 and 4 would be expected to approach a constant ratio. In contrast, the statistical factor for process 3 should be much greater because two bonds are broken and three separate species are produced so that the number of ways of partitioning energy in the products is increased. Thus if the

proton affinity of B is sufficiently high so that all three reaction pathways are exothermic, process 3 would be expected to dominate. From this model, Fig. 3 is understood as follows. For species slightly more basic than H_2O, only reaction 2 is exothermic. As the proton affinity of B increases, reaction 4 becomes accessible and, due to contributions from the thermal energy of the reactants, BH^+ production is observed below the calculated threshold. Since the threshold for reaction 4 is 5.0 kcal $mole^{-1}$ less than for reaction 3, the latter process is not expected to contribute until the proton affinity of B increases somewhat above the observed threshold for BH^+ production. Since statistical factors for the processes 2 and 4 are similar, $BH(OH_2)^+$ production continues until 14 kcal mol^{-1} above the observed threshold for reaction 2. At this point, reaction 3 becomes the dominant pathway yielding BH^+ and reactions 2 and 4 are curtailed by unfavorable frequency factors. Hence, production of $H(OH_2)_2^+$ is prevented, as observed.

Studies of this nature would be hampered at higher pressure because $BH(OH_2)^+$ will be produced from BH^+ by direct association, eq. 25, making determination of the product ratios difficult. Thus,

$$BH^+ + H_2O \xrightarrow{[M]} BH(OH_2)^+ \qquad (25)$$

low pressure trapped ion ICR experiments where termolecular processes can be avoided are particularly suited for such studies.

Acknowledgment

This research was supported in part by the Army Research Office.

References

(1) Berman, D. W.; and Beauchamp, J. L. J. Phys. Chem. 1980, 84, 2233.

(2) Berman, D. W.; and Beauchamp, J. L. J. Am. Chem. Soc., to be submitted.

(3) Clair, R. L.; and McMahan, T. B. Can. J. Chem., 1980, 58, 863.

(4) See for example: Cunningham, A. J.; Payzant, J. D.; and Kebarle, P. J. Am. Chem. Soc., 1972, 94, 7627.

(5) Beauchamp, J. L. Annu. Rev. Phys. Chem., 1971, 22, 527.

(6) Beauchamp, J. L.; Holtz, D.; Woodgate, S. D.; and Patt, S. L. J. Am. Chem. Soc., 1972, 94, 2798.

(7) McMahon, T. B.; and Beauchamp, J. L. Rev. Sci. Instrum. 1972, 43, 509.

(8) Wolf, J. F.; Staley, R. H.; Koppel, I.; Taagepera, M.; McIver, R. T.; Beauchamp, J. L.; and Taft, R. W. J. Am. Chem. Soc. 1977, 99, 5417.

(9) Kebarle, P. Ann. Rev. Phys. Chem., 1977, 28, 445.

(10) Curtis, L. A.; Frurip, D. L.; and Blander, M. Chem. Phys. Lett. 1978, 54, 575.

(11) $D(H_2O\text{-}H_2O) = 5.0$ kcal $mol^{-1} \pm 1$ at 298° K is derived from $D(H_2O\text{-}H_2O) = 5.5$ kcal mol^{-1} at 0° K obtained in ref. 10 by accounting for internal energy contributions at 298° K.

(12) R. W. Taft, "Proton Transfer Reactions", (Caldin, E. F.; and Gold, V. ed.), Chapman and Hall, London, 1975.

References (continued)

(13) Yamdagni, R.; and Kebarle, P. J. Am. Chem. Soc., 1976, 98 1320.

(14) For a general review see: Hartman, K. N.; Lias, S.; Ausloos, P.; Rosenstock, H. M.; Schroyer, S. S.; Schmidt, C.; Martinsen, D.; and Milne, G. W. A. "A Compendium of Gas Phase Basicity and Proton Affinity Measurements", NBSIR 79-1777, (U.S. Gov't. Printing Office, 1979).

(15) Ceyer, S. T.; Tiedemann, P. W.; Mahan, B. H.; and Lee, Y.T. J. Chem. Phys. 1979, 70, 14.

(16) Rowlinson, J.S. Discuss. Faraday Soc., 1949, 45, 974.

(17) Ng, C. Y.; Trevor, D. J.; Tiedemann, P. W.; Ceyer, S. T.; Kronebusch, P. L.; Mahan, B. H.; and Lee, Y. T. J. Chem. Phys., 1977, 67, 4235.

(18) Kebarle, P.; Searles, S. K.; Zolla, A.; Scarborough, J.; and Arshadi, M. J. Am. Chem. Soc., 1967, 89, 1967.

(19) Meotner, M.; and Field, F. H. J. Am. Chem. Soc., 1977, 99, 998.

(20) Curtiss, L. A.; Frurip, D. J.; and Blandu, M. J. Chem. Phys. 1979, 71, 2703.

(21) Bouchez, P.; Block, R.; and Jansen, L. Chem. Phys. Lett., 1979, 65, 212.

(22) See for example: Robinson, P. J.; and Holbrook, K. A. "Unimolecular Reactions:, Wiley-Interscience, New York, 1972.

References (continued)

(23) See for example: Dunbar, R. C. Spectrochemica Acta, 1975, 31A, 797.

(24) Stull, P. R.; and Prophet, H. "JANAF Thermochemical Tables," 2nd Ed. NSRDS-NBS37 (U.S. Gov't. Printing Office, Washington, D.C. 1971).

(25) See for example: Newton, M. D. J. Chem. Phys. 1977, 67, 5535.

CHAPTER IV

PHOTOIONIZATION THRESHOLD MEASUREMENTS FOR CF_2 LOSS FROM THE MOLECULAR IONS OF PERFLUOROPROPYLENE, PERFLUOROCYCLOPROPANE, AND TRIFLUOROMETHYLBENZENE. THE HEAT OF FORMATION OF CF_2 AND CONSIDERATION OF THE POTENTIAL ENERGY SURFACE FOR INTERCONVERSION OF $C_3F_6^+$ ISOMERIC IONS

PHOTOIONIZATION THRESHOLD MEASUREMENTS FOR CF_2 LOSS FROM THE MOLECULAR IONS OF PERFLUOROPROPYLENE, PERFLUOROCYCLOPROPANE, AND TRIFLUOROMETHYLBENZENE. THE HEAT OF FORMATION OF CF_2 AND CONSIDERATION OF THE POTENTIAL ENERGY SURFACE FOR INTERCONVERSION OF $C_3F_6^+$ ISOMERIC IONS

D. W. BERMAN, D. S. BOMSE and J. L. BEAUCHAMP

Contribution No. from the Arthur Amos Noyes Laboratory of Chemical Physics, California Institute of Technology, Pasadena, California 91125 (U. S. A.)

(First received

Abstract

Photoionization of perfluoropropylene, perfluorocyclopropane, and trifluoromethylbenzene yield onsets for ions formed by loss of a CF_2 neutral fragment. $\Delta H^\circ_{f_{298}}(CF_2) = -44.2 \pm 1$ kcal mole^{-1} is derived from these thresholds. Earlier determinations of $\Delta H^\circ_{f_{298}}(CF_2)$ are reinterpreted using updated thermochemical values and found to be in excellent agreement with this work. The heat of formation of neutral perfluorocyclopropane, $\Delta H^\circ_{f_{298}}(c\text{-}C_3F_6) = -233.8 \pm 2$ kcal mole^{-1} is derived from the onset of $C_2F_4^+$ and the $\Delta H^\circ_f(CF_2)$ value cited. This compares favorable with the heat of formation of perfluorocyclopropane derived from measurements of the forward and reverse enthalpies of activation for the addition of CF_2 to C_2F_4. The energetics of interconversion of perfluoropropylene and perfluorocyclopropane are described for both the neutrals and their molecular ions.

INTRODUCTION

The heat of formation of CF_2 has been a subject of considerable controversy [1-5], with reported values ranging between -6.3 and -50 kcal mol^{-1} [3]. Because photoionization studies are capable of yielding precise thermochemical information [6], studies of fluorinated compounds yielding a CF_2 fragment upon photoionization might provide useful additional information concerning $\Delta H_f^0(CF_2)$. A well-known molecular ion decomposition pathway of species bearing a trifluoromethyl substituent is the rearrangement process 1 [7].

$$RCF_3 + h\nu \rightarrow [R\text{-}CF_3^+]^* \rightarrow RF^+ + CF_2 \qquad (1)$$

Measurement of the ionization threshold for process (1) can yield the heat of formation of CF_2. However, because knowledge of the heats of formation of RCF_3, RF, and the adiabatic ionization potential of RF would be required to calculate $\Delta H_f^0(CF_2)$, a judicious choice of RCF_3 is necessary. Results of a photoionization study of perfluoropropylene and trifluoromethylbenzene are reported in the present work. Heats of formation and ionization energetics of the pertinent species are available from earlier work employing rotating bomb calorimetry [8], photoelectron spectroscopy [9], and UV spectroscopy [10]. In addition, we have examined the threshold formation of CF_2 from perfluorocyclopropane. In this case, the heat of formation of the precurser is derived. The energetics of rearrangement and decomposition processes involving the two neutral C_3F_6 isomers and their molecular ions are discussed.

EXPERIMENTAL

The photoionization mass spectrometer employed in these studies has been documented previously [11, 12]. For a source of photons with energies between 8 and 13 eV, a high voltage d. c. discharge was used to generate the characteristic many-lined spectrum of hydrogen (1600-950 Å). An rf discharge generating the Hopfield continuum of helium (950-700 Å) was the light source for energies up to 18 eV. The monochromator was set for 1. 5 Å fwhm resolution. The repellor voltage was maintained at + 0. 2 V yielding ion residence times of ~25 μsec. Typical sample pressures were 1. 0 - 4. 0 $\times$ 10^{-4} Torr. All data were collected at ambient temperature (25° C).

Perfluorocyclopropane was provided by Professor J. D. Roberts. Perfluoropropylene and trifluoromethylbenzene were available from commercial sources. These substances were used without further purification except for several freeze-pump-thaw cycles to remove non-condensable gases. No impurities were detected by mass spectrometry.

RESULTS

Perfluoropropylene

Relative photoionization efficiency curves for the $C_3F_6^+$ molecular ion and $C_2F_4^+$ fragment of perfluoropropylene are presented in Fig. 1. Steplike structure on the parent ion curve

FIGURE 1. Photoionization efficiency curves for $C_3F_6^+$ and $C_2F_4^+$ in perfluoropropylene at 1.0×10^{-4} torr.

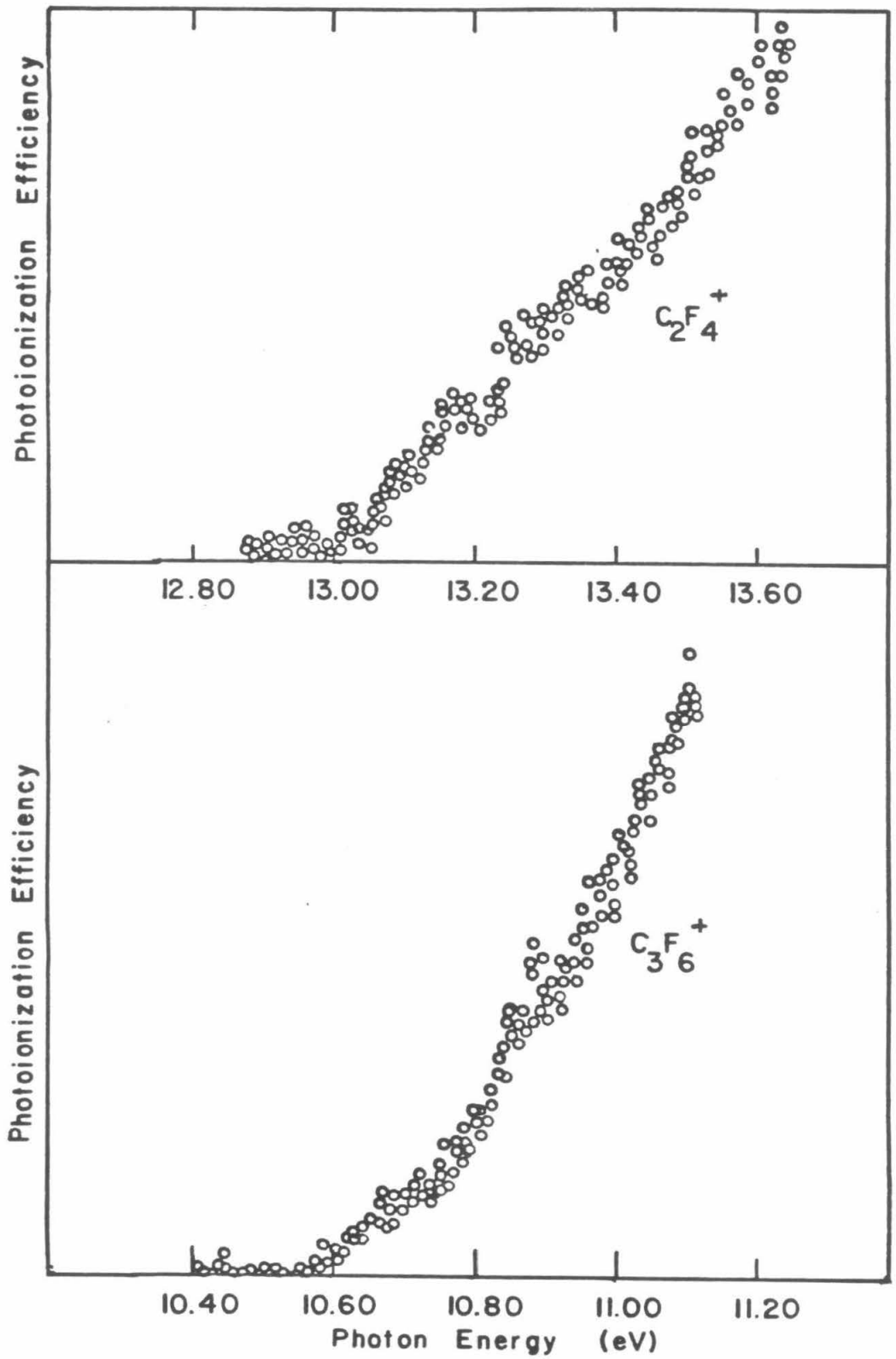
Photoionization Efficiency
$C_2F_4^+$
12.80
13.00
13.20
13.40
13.60
Photoionization Efficiency
$C_3F_6^+$
10.40
10.60
10.80
11.00
11.20
Photon Energy (eV)

reflects contributions to the total molecular ion intensity from vibrationally excited $C_3F_6^+$. The first rise at 1170. 2 Å yields an adiabatic ionization threshold of 10. 60 ± 0. 03 eV for $C_3F_6^+$ in agreement with 10. 62 eV from the photoelectron spectrum [13].

A sharp onset at 13. 04 ± 0. 03 eV is observed for $C_2F_4^+$ formation, Fig. 1. Interestingly, the efficiency curve of $C_2F_4^+$ also exhibits steplike structure. Such features are unusual for fragment ions because excess internal energy in the parent precurser can contribute to formation of translationally and rotationally excited fragments, so that the probability for decomposition is not significantly increased as a new vibrational mode becomes accessible [14, 15]. The discontinuities on the $C_2F_4^+$ efficiency curve therefore suggest strong predissociative coupling of parent ion states with fragment ion states. A photoion-photoelectron coincidence study might provide further evidence for such behavior. A summary of ionization and appearance thresholds measured in this and related work is presented in Table 1.

Trifluoromethylbenzene

Figure 2 presents photoionization onsets for $C_6H_5CF_3^+$ and $C_6H_5F^+$ derived from trifluoromethylbenzene. The parent ion exhibits a sharp onset yielding an adiabatic ionization potential of 9. 69 ± 0. 03 eV, in excellent agreement with the previously reported values of 9. 685 ± 0. 005 eV [10] and 9. 68 ± 0. 02 eV [16]. The onset for $C_6H_5F^+$ formation, process (1), is found to be 12. 40 ± 0. 1 eV. This result is subject to greater uncertainty than other

TABLE 1

Measured Photoionization onsets and derived heats of formation from this and related work

Species	Ion	Neutral Fragment	IP[a]	AP[a]	$\Delta H^0_{f_{298}}$ [b]
C_3F_6					-268.9[c]
	$C_3F_6^+$		10.60 ± 0.03[d]		- 24.5 ± 1[d]
			10.62 ± 0.03[e]		
	$C_2F_4^+$	(CF_2)		13.04 ± 0.03[d]	
		CF_2			- 44.2 ± 1[d]
c-C_3F_6					-233.8 ± 2[d]
	$C_3F_6^+$		11.18 ± 0.03[d]		(24 ± 2)[d]
			11.20 ± 0.03[f]		
	$C_2F_4^+$	(CF_2)		11.52 ± 0.03[d]	
		CF_2			
$C_6H_5CF_3$					-143.4[g]
	$C_6H_5CF_3^+$		9.69 ± 0.03[d]		80.1 ± 1[d]
			9.685 ± 0.005[h]		
			9.68 ± 0.02[j]		
	$C_5H_5F^+$	(CF_2)		12.40 ± 0.1[d]	
		CF_2			- 41.8 ± 4[d]
C_2F_4					-157.4[g]
	$C_2F_4^+$		10.12 ± 0.01[k]		76.0[k]
C_6H_5F					- 27.9[g]
	$C_6H_5F^+$		9.200 ± 0.005[h]		184.4[h]

TABLE 1 (Continued)

---

[a]Units are eV.

[b]Units are kcal mol^{-1}

[c]W. M. D. Bryant, J. Polym. Sci., 56 (1962) 277.

[d]This work.

[e]Ref. 13.

[f]Ref. 17.

[g]Ref. 8.

[h]Ref. 10.

[j]Ref. 16.

[k]Ref. 9.

FIGURE 2. Photoionization efficiency curves for $C_6H_5CF_3^+$ and $C_6H_5F^+$ from trifluoromethylbenzene at 4.0×10^{-4} torr.

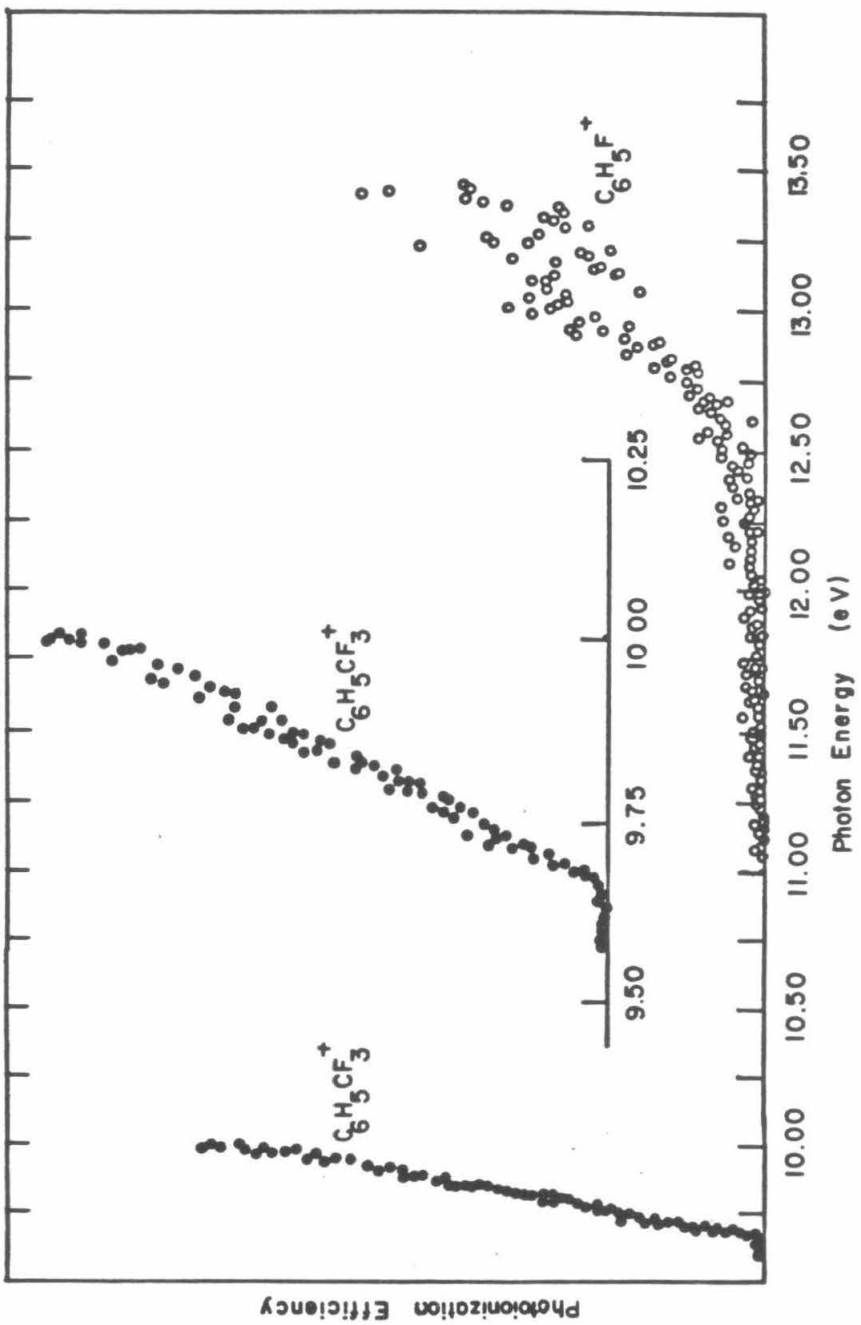
Photoionization Efficiency
Photon Energy (eV)
10.00
10.50
11.00
11.50
12.00
12.50
13.00
13.50
9.50
9.75
10.00
10.25
$C_6H_5CF_3^+$
$C_6H_5CF_3^+$
$C_6H_5F^+$

measurements presented here because the $C_6H_5F^+$ signal intensity is limited by lack of light from either the hydrogen or helium sources at energies near the threshold for formation of $C_6H_5F^+$ from $C_6H_5CF_3$.

Perfluorocyclopropane

Relative photoionization efficiency curves for the $C_3F_6^+$ molecular ion and $C_2F_4^+$ fragment of perfluorocyclopropane are presented in Fig. 3. The measured parent ion onset, 11.18 ± 0.3 eV, is in accord with an unpublished photoelectron spectrum [17]. Unlike fluorinated propylene, the cyclic parent ion does not exhibit a sharp threshold. Lack of a sharp onset for parent ions suggests a major structural rearrangement takes place upon ionization so that Franck-Condon factors are small for transitions from the ground state neutral to the ground state ion. In this system, the 11.52 ± 0.03 eV threshold measured for $C_2F_4^+$ formation is sharper than the molecular ion onset.

DISCUSSION

Heat of formation of CF_2

As with many fluorinated organic molecules [1, 4, 8], the thermodynamic properties of neutrals discussed in this paper have not been sufficiently well characterized to permit or require the derivation of 0°K appearance thresholds. Therefore, all onsets and related thermochemical quantities will be calculated and reported at

FIGURE 3. Photoionization efficiency curves for $C_3F_6^+$ and $C_2F_4^+$ from perfluorocyclopropane at 2.0×10^{-4} torr.

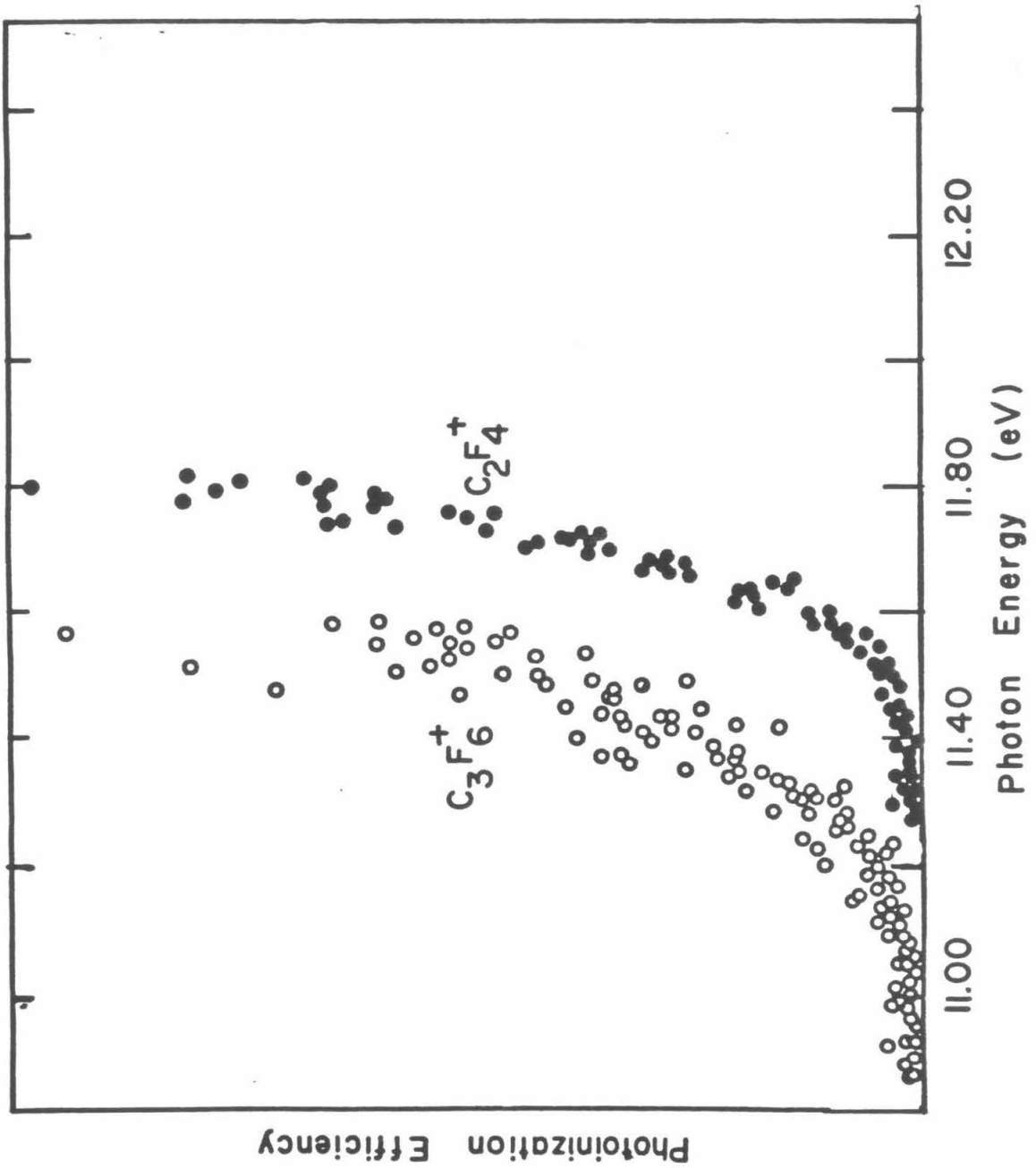
Photoionization Efficiency
11.00
11.40
11.80
12.20
Photon Energy (eV)
$C_2F_4^+$
$C_3F_6^+$

298°K. Using the 13.04 eV onset of $C_2F_4^+$ from perfluoropropylene with $\Delta H^0_{f298}(C_2F_4)$ and $IP(C_2F_4)$ presented in Table 1, $\Delta H^0_{f_{298}}(CF_2)$ = -44.2 kcal mol^{-1} can be calculated. When the updated 174 ± 2 kcal mol^{-1} H_2O proton affinity [18] is employed, an identical value of $\Delta H^0_{f_{298}}(CF_2)$ = -44.3 ± 1 kcal mol^{-1} is derived from an earlier ICR investigation [4]. Generally, if earlier measurements of $\Delta H^0_f(CF_2)$ are reinterpreted using the set of neutral thermochemical data presented in Table 1, excellent agreement obtains among a large number of determinations. Corrected values of $\Delta H^0_{f_{298}}(CF_2)$ are presented in Table 2. Experimental methods of determination are listed beside each entry in the table. The best estimate for $\Delta H^0_{f_{298}}(CF_2)$ is -43.8 kcal mol^{-1}.

Heat of formation of perfluorocyclopropane

Using thermochemical quantities from Tables 1 and 2, the 11.52 eV threshold for formation of $C_2F_4^+$ from c-C_3F_6 can be combined with $\Delta H^0_{f_{298}}(C_2F_4^+)$ = 76.0 kcal mol^{-1} and $\Delta H^0_{f_{298}}(CF_2)$ = -43.8 kcal mol^{-1} to yield $\Delta H^0_{f_{298}}$(c-C_3F_6) = -233.5 ± 2 kcal mol^{-1}. Atkinson et al. [19] measured the forward and reverse enthalpies of activation for decomposition of c-C_3F_6, equation (2). The reported values were

$$c\text{-}C_3F_6 \rightarrow CF_2 + C_2F_4 \qquad (2)$$

39 kcal mol^{-1} and 8 kcal mol^{-1}, respectively. Using the 31 kcal mol^{-1} difference as the enthalpy of reaction for equation (2), then $\Delta H^0_{f_{298}}$(c-C_3F_6) = -232.2 ± 2 kcal mol^{-1} can be derived employing

TABLE 2

Heat of formation of CF_2 at 298°K

$\Delta H^0_{f_{298}}(CF_2)$[a]	Technique[b]
-44.2 ± 1	photoionization of C_3F_6[c]
(-41.8 ± 4)	photoionization of $C_6H_5CF_3$[d]
-41.7 ± 2	photoionization of C_2F_4[e]
-44.3 ± 2	ICR measurement of $PA(CF_2)$[f]
-44.1 ± 2	thermal decomposition of CF_3H, $CHClF_2$, C_2F_4[g]
-45.4 ± 2	thermal equilibrium of $C_2F_4 \rightleftharpoons CF_2 + CF_2$[h]
-44.5 ± 1	thermal equilibrium of $C_2F_4 \rightleftharpoons CF_2 + CF_2$[j]
-41.2 ± 2	thermal equilibrium of $C_2F_4 \rightleftharpoons CF_2 + CF_2$[k]
-42.3 ± 1	thermal equilibrium of $C + 2F \rightleftharpoons CF_2$[l]
-43.5 ± 2	third law calculation[m]
-42 ± 4	thermal equilibrium of $CHF_2Cl \rightleftharpoons CF_2 + HCl$[n]
-42.6 ± 1	thermal decomposition of C_2F_4[o]
-43.8 ± 2	weighted average of above determinations

[a] Units are kcal mol^{-1}.

[b] Results of reported works are recalculated using thermochemical values from Table 1.

[c] This work.

[d] This work. As noted in text, lack of light leads to a large uncertainty in the value presented here.

TABLE 2 (Continued)

---

[e]Ref. 9. $IP(CF_2)$ = 11.42 eV from J. M. Dyke, L. Golub, N. Jonathan, A. Morris and M. Okuda, J. Chem. Soc. Faraday Trans. II, 70 (1979) 1828 is employed. If $IP(CF_2)$ = 11.7 eV from I. P. Fisher, J. B. Hower and F. P. Lossing, J. Am. Chem. Soc., 87 (1965) 957 is used instead, $\Delta H_f^0(CF_2)$ = -43.4 ± 2 kcal mol^{-1} is derived. There may be problems with this onset because several other fragment ions from C_2F_4 appear at lower energies so that the threshold for formation of CF_2^+ is not sharp.

[f]Ref. 4. This assumes $PA(H_2O)$ = 174 ± 2 kcal mol^{-1} from ref. 18. Also, $\Delta H_f^0(CHF_2^+)$ = 142.4 kcal mol^{-1} is used from R. J. Blint, T. B. McMahan and J. L. Beauchamp, J. Am. Chem. Soc., 96 (1974) 1269.

[g]Ref. 5. $\Delta H_f^0(CF_3H)$ = -166.6, $\Delta H_f^0(CHClF_2)$ = -115.1 are from ref. 1.

[h]A. P. Modica and J. E. LeGraff, J. Chem. Phys., 43 (1965) 3383.

[j]Ref. 1.

[k]K. F. Zmboo, O. M. Ury and J. L. Margrave, J. Am. Chem. Soc., 90 (1968) 5090.

[l]M. Farber, M. A. Frish and H. C. Ko, Trans. Faraday Soc., 65, (1969) 3202.

[m]Ref. 1. The data from references h, j, k, and l were combined and a third law calculation was applied to the entire set.

[n]J. W. Edwards and P. A. Small, Ind. Eng. Chem. Fundamentals, 4 (1965) 396. $\Delta H_f^0(CF_2HCl)$ and $\Delta H_f^0(HCl)$ are from ref. 1.

[o]F. W. Dalby, J. Chem. Phys., 41 (1964) 2297.

$\Delta H^0_{f_{298}}(CF_2)$ = -43. 8 kcal mol^{-1} and $\Delta H^0_f(C_2F_4)$ = -157. 4 kcal mol^{-1} from Table 1. Excellent agreement between these two determinations provide confidence in the accuracy of -233 ± 2 kcal mol^{-1} for the heat of formation of perfluorocyclopropane.

Stability of the perfluorocyclopropane molecular ion

Figure 4 is constructed from thermodynamic quantities presented in Table 1. This figure represents a reaction coordinate diagram for rearrangement and decomposition of C_3F_6 neutral and ion isomers. Since thermolysis of c-C_3F_6 yields only C_2F_4 and CF_2, the barrier to rearrangement of c-C_3F_6 must be greater than the 39 kcal mol^{-1} barrier measured for decomposition [19]. Neutral perfluorocyclopropane is stable, occupying a minimum in the energy surface of C_3F_6. The situation may be different for the c-C_3F_6 ion, however. The 0. 34 eV difference between measured adiabatic onsets for $C_3F_6^+$ and $C_2F_4^+$ formation from c-C_3F_6 neutral represents an upper limit of 8 kcal mol^{-1} by which the cyclic molecular ion can be bound with respect to dissociation. But the barrier to rearrangement may be smaller. $C_3F_6^+$ ions formed from c-C_3F_6 by impact of 20 eV electrons totally rearrange to a 48 kcal mol^{-1} more stable acyclic structure [20]. The lack of a sharp onset at threshold for photoionization of cyclo-C_3F_6 suggests a major structural rearrangement is also occurring during this process. Thus, c-$C_3F_6^+$ probably does not lie at a potential minimum in the $C_3F_6^+$ ion energy surface but is unstable toward rearrangement to an acyclic species.

FIGURE 4. Reaction coordinate diagram for C_3F_6 and $C_3F_6^+$. Relevant thermochemical quantities can be found in Table I and ref. 19.

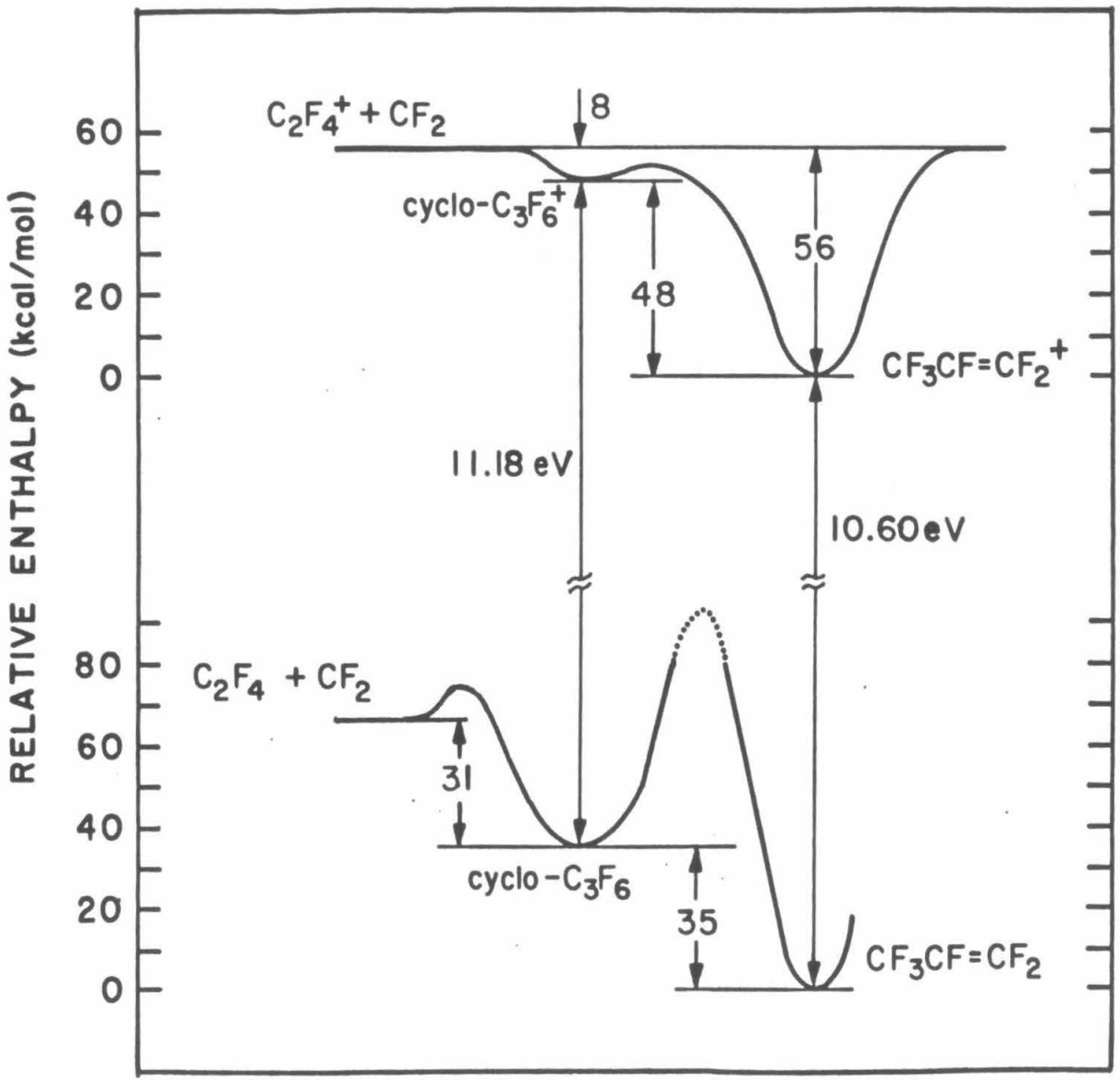
RELATIVE ENTHALPY (kcal/mol)
60
40
20
0
80
60
40
20
0
$C_2F_4^+ + CF_2$
8
cyclo-$C_3F_6^+$
48
56
$CF_3CF=CF_2^+$
11.18 eV
10.60eV
$C_2F_4 + CF_2$
31
cyclo-C_3F_6
35
$CF_3CF=CF_2$

REFERENCES

1 See discussion: P. R. Stull and H. Prophet, "JANAF Thermochemical Tables", 2nd Ed. NSRDS-NBS, 37 (1971) U. S. Government Printing Office, Washington, D. C.

2 E. N. Okafo and E. Whittle, J. Chem. Soc. Faraday Trans. 1, 70 (1974) 1366.

3 J. Heiklen, Adv. Photochem., (1969) 7.

4 J. Vogt and J. L. Beauchamp, J. Am. Chem. Soc., 97 (1975) 6682.

5 K. P. Schug, H. Gg. Wagner and F. Zabel, Ber. Bunsenges. Phys. Chem., 83 (1978) 167.

6 See for example: W. A. Chupka in "Ion Molecule Reactions", Vol. 1, J. L. Franklin, ed., Plenum, New York, 1972, Chapter 3.

7 See for example: F. W. McLafferty, "Interpretation of Mass Spectra", 2nd Ed., W. A. Benjamin, Inc., London, 1973, p. 65.

8 J. R. Lacher and H. A. Skinner, J. Chem. Soc. A, (1968) 1034.

9 T. A. Walter, C. Lifshitz, W. A. Chupka and J. Berkowitz, J. Chem. Phys., 51 (1969) 3531.

10 V. J. Hammond, W. C. Price, J. P. Teegan and A. D. Walsh, Discuss. Faraday Soc., 9 (1950) 53.

11 P. R. LeBreton, A. D. Williamson, J. L. Beauchamp and W. T. Huntress, J. Chem. Phys., 62 (1975) 1623.

12 A. D. Williamson, Ph. D. Dissertation, California Institute of Technology, 1975.

13 B. S. Freiser and J. L. Beauchamp, J. Am. Chem. Soc., 96 (1974) 6260.

14 W. A. Chupka, J. Chem. Phys., 54 (1970) 1936.

15 Ibid., 30 (1959) 191.

16 K. Watanabe, T. Nokayama and J. Mottl, J. Quantum Spectr. Radiative Transfer, 2 (1962) 369.

17 W. A. Chupka and J. L. Beauchamp, unpublished results.

18 F. A. Houle and J. L. Beauchamp, J. Am. Chem. Soc., 101 (1979) 4067.

19 B. Atkinson and D. McKeagar, Chem. Comm., (1966) 189.

20 D. S. Bomse, D. W. Berman and J. L. Beauchamp, J. Am. Chem. Soc., submitted.

CHAPTER V

ION CYCLOTRON RESONANCE AND PHOTOIONIZATION INVESTIGATIONS OF THE THERMOCHEMISTRY AND REACTIONS OF IONS DERIVED FROM CF_3I

ION CYCLOTRON RESONANCE AND PHOTOIONIZATION INVESTIGATIONS OF THE THERMOCHEMISTRY AND REACTIONS OF IONS DERIVED FROM CF_3I

D. WAYNE BERMAN, L. R. THORNE and J. L. BEAUCHAMP

Arthur Amos Noyes Laboratory of Chemical Physics,
Department of Chemistry, California Institute of Technology,
Pasadena, California 91125

(Received)

Abstract

The techniques of ion cyclotron resonance spectroscopy and photoionization mass spectrometry are used to investigate the thermochemistry and ion-molecule reactions of ions derived from CF_3I. Reaction sequences are identified and rate constants measured for reactive fragment ions using trapped ion techniques at low pressure ($0.5 - 1.0 \times 10^{-7}$ torr). Only bimolecular reactions are observed, and the results are contrasted with previous experiments at high pressures. Photoionization thresholds of 10.32 and 11.36 eV are measured for the molecular ion and CF_3^+ fragments respectively. The latter threshold gives $\Delta H_{f_0}^\circ$ $(CF_3^+) = 98.3 \pm 1$ kcal mole^{-1} or $\Delta H_{f_{298}}^\circ$ $(CF_3^+) = 97.6$ kcal mole^{-1}, which are shown to be in excellent agreement with independent determinations of this quantity.

INTRODUCTION

The gas phase ion chemistry of CF_3I has been investigated using time of flight mass spectrometry with ion cyclotron double resonance to 'identify' reaction pathways [1]. The latter experiments are generally conducted at pressures several orders of magnitude lower than those employed in time of flight studies. We report here an investigation of the gas phase ion chemistry of CF_3I utilizing trapped ion cyclotron resonance techniques. The present results differ significantly from the earlier report in that only bimolecular processes are important; termolecular reactions leading to cluster formation are not observed.

In characterizing the thermochemistry of ionic species derived in this work, it became apparent that large discrepancies persist in the heat of formation of CF_3^+ derived from photoionization of CF_3X (process 1), where X = F [2, 3, 4], Cl [2, 3, 5, 6], Br [3], and I [3].

$$CF_3X + h\nu \rightarrow CF_3^+ + X \qquad (1)$$

We have thus determined photoionization efficiency curves for the molecular ion and CF_3^+ fragment from CF_3I. The present results provide information helpful in interpreting the results of recent studies of the single photon [7] and multiphoton infrared laser [8] dissociation of CF_3I^+.

EXPERIMENTAL

ICR instrumentation and techniques used in these studies have been previously described in detail [9-11]. All experiments were performed at ambient temperature (20-25° C). Pressures were measured with a Schulz-Phelps type ionization gauge calibrated against an MKS Instruments Baratron Model 90H1-E capacitance manometer. Based on these pressure measurements, reported reaction rates are accurate to within ± 20%.

The photoionization mass spectrometer employed for this work has been documented previously [12,13]. A high voltage d.c. discharge was used to generate the characteristic many-lined spectrum of hydrogen (950-1600 Å) for the light source in these studies. The monochromator was set for 1 Å fwhm resolution. Typical sample pressures were in the range $5.0 - 20.0 \times 10^{-5}$ torr. Spectra were collected at several repeller voltages between 0.5 and 0.2 v such that ion residence times varied between 10 and 250 μsec, respectively. The source was operated at ambient temperature (25° C).

CF_3I was obtained from commercial sources and used without further purification except for several freeze-pump-thaw cycles to remove air. Mass spectra showed no detectable impurities.

RESULTS

Ion Chemistry of CF_3I.

Abundant ions formed by 70 eV electron impact in CF_3I below 10^{-6} torr are CF_3I^+ (37.6%), CF_2I^+ (11.5%), I^+ (32.9%), and CF_3^+ (18.0%). As depicted in Fig. 1, CF_3^+ and I^+ react with neutral CF_3I, while CF_3I^+ and CF_2I^+ are unreactive, persisting at long times. Disappearance of I^+ is attributed to two pathways, reactions (2) and (3), CF_3^+ decays via reaction (4). These are confirmed by double resonance techniques.

$$I^+ + CF_3I \begin{cases} \rightarrow CF_3^+ + I_2 & (2) \\ \rightarrow CF_3I^+ + I & (3) \end{cases}$$

$$CF_3^+ + CF_3I \rightarrow CF_2I^+ + CF_4 \qquad (4)$$

Measured rate constants and calculated heats of reaction for these processes are given in Table I.

The present results differ somewhat from previsouly reported ion chemistry of CF_3I [1]. Specifically, the previous study did not identify reaction (2) as being responsible, in part, for the disappearance of I^+. Nor do we observe the ions I_2^+, $CF_3I_2^+$ of $(CF_3I)_2^+$ reported in the time of flight experiments. The former species were attributed to bimolecular reactions involving I^+ and CF_3I^+, respectively, as the reactant ions. If these reactions indeed occur then they must reflect different internal state distributions or reactant ion translational energy distributions which distinguish the two methods. It was also reported [1] that collision induced dissociation of CF_3I^+ occurs to yield CF_3^+;

FIGURE 1. Variation of ion abundance with time for CF_3I at 1.7×10^{-7} torr following a 10 msec, 70 eV electron pulse. Markers show observed data, solid lines are calculated from the rate constants in Table 1.

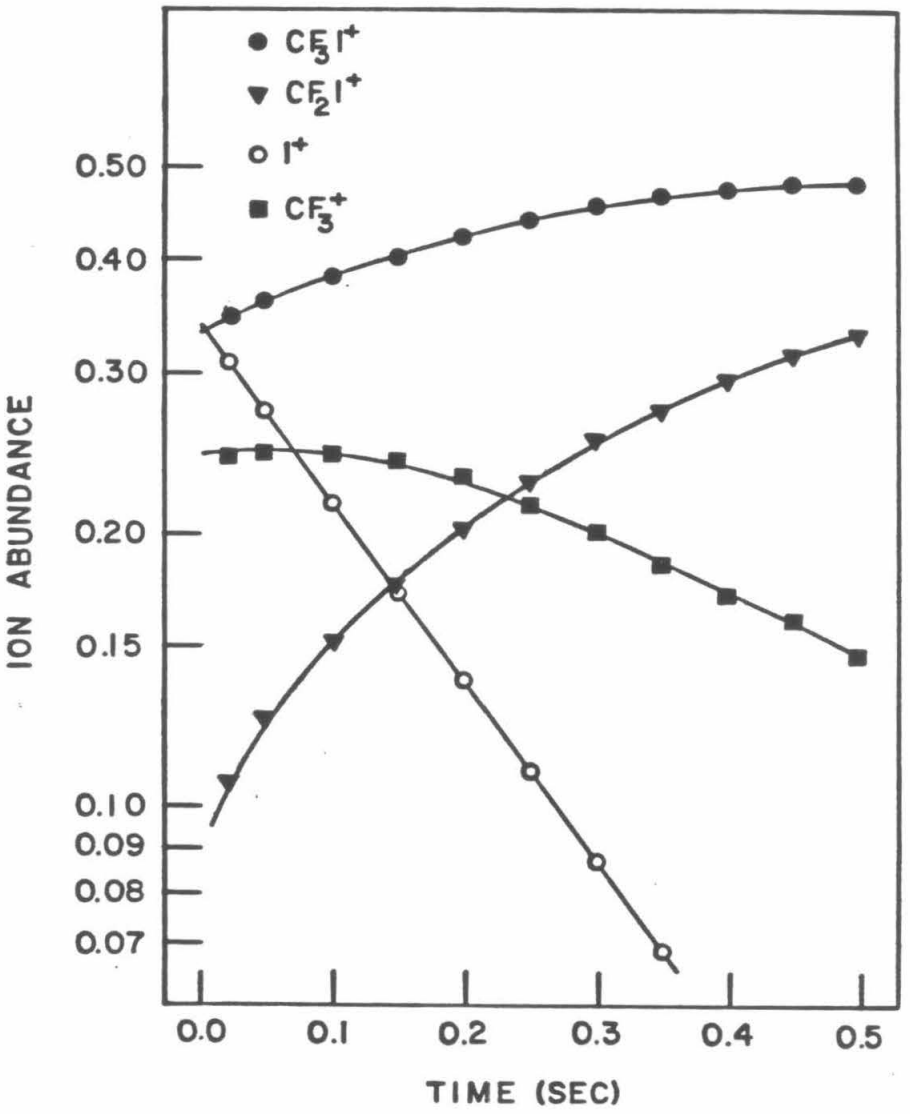
● CF_3I^+
▼ CF_2I^+
○ I^+
■ CF_3^+
ION ABUNDANCE
0.50
0.40
0.30
0.20
0.15
0.10
0.09
0.08
0.07
0.0
0.1
0.2
0.3
0.4
0.5
TIME (SEC)

TABLE I

Ion-molecule reactions of CF_3I

	Reaction	$\Delta H^\circ_{f_{298}}$ [a]	k[b]
(1)	$I^+ + CF_3I \rightarrow CF_3^+ + I_2$	-13.9[c]	3.5
(2)	$I^+ + CF_3I \rightarrow CF_3I^+ + I$	-3.0[d]	3.9
(4)	$CF_3^+ + CF_3I \rightarrow CF_2I^+ + CF_4$	-4.0[e]	4.8

a Units are kcal/mole^{-1}

b Units are 10^{-10} cm^3 molecule^{-1} sec^{-1}. Obtained from a least squares fit of the data shown in Fig. 1.

c Obtained from the thermochemical data cited in Table III and Ref. 6.

d Obtained from the difference between IP(I) = 10.45 eV and IP(CF_3I) = 10.32 eV cited in Ref. 16 and Table III, respectively.

e Obtained from thermochemical data cited in Table III and Ref. 16.

double resonance experiments indicate no evidence for this process in the pressure range $0.5 - 1.0 \times 10^{-7}$ torr.

Photoionization Mass Spectrometry of CF_3I

Relative photoionization efficiency curves for the molecular ion CF_3I^+ and fragment CF_3^+ are presented in Fig. 2. No other fragment ions are observed over the useful energy range of the hydrogen many-lined source (up to 13.1 eV). The photoelectron spectrum of CF_3I [14] (Fig. 3) shows the two spin orbit components of the ground electronic state of CF_3I^+. In Fig. 2, the $^2E_{\frac{1}{2}}$ ionic state becomes accessible as the photon energy is increased beyond 10.9 eV [14], and a second 0.5 eV wide step in the CF_3I^+ photoionization efficiency curve reflects the contribution of this state to total molecular ion intensity. In contrast to the results presented by Noutary [3], the onset of CF_3^+ is sufficiently sharp to determine an accurate ionization threshold. The value measured at 298° K, 11.27 eV is corrected to 0° K by subtracting the average thermal energy content of the parent neutral. This gives 11.36 ± 0.02 eV. In an attempt to determine the origin of the discrepancy between our results and those of Noutary [3], several possibilities were explored. To check for the presence of a kinetic shift, measurements were made at several repeller plate voltages between 0.5 and 0.02 V, yielding ion residence times between 10 and 250 μsec respectively. The onset for both CF_3I^+ and CF_3^+ remain unchanged over this range of residence times, demonstrating the absence of a kinetic shift for the fragment ion. The ion pair process depicted in Eq. (5) might contribute to the tailing observed for CF_3^+ in

FIGURE 2. Photoionization efficiency curves for CF_3I^+ and CF_3^+ in CF_3I. Inset presents an expanded view of the onset region of the CF_3^+ curve.

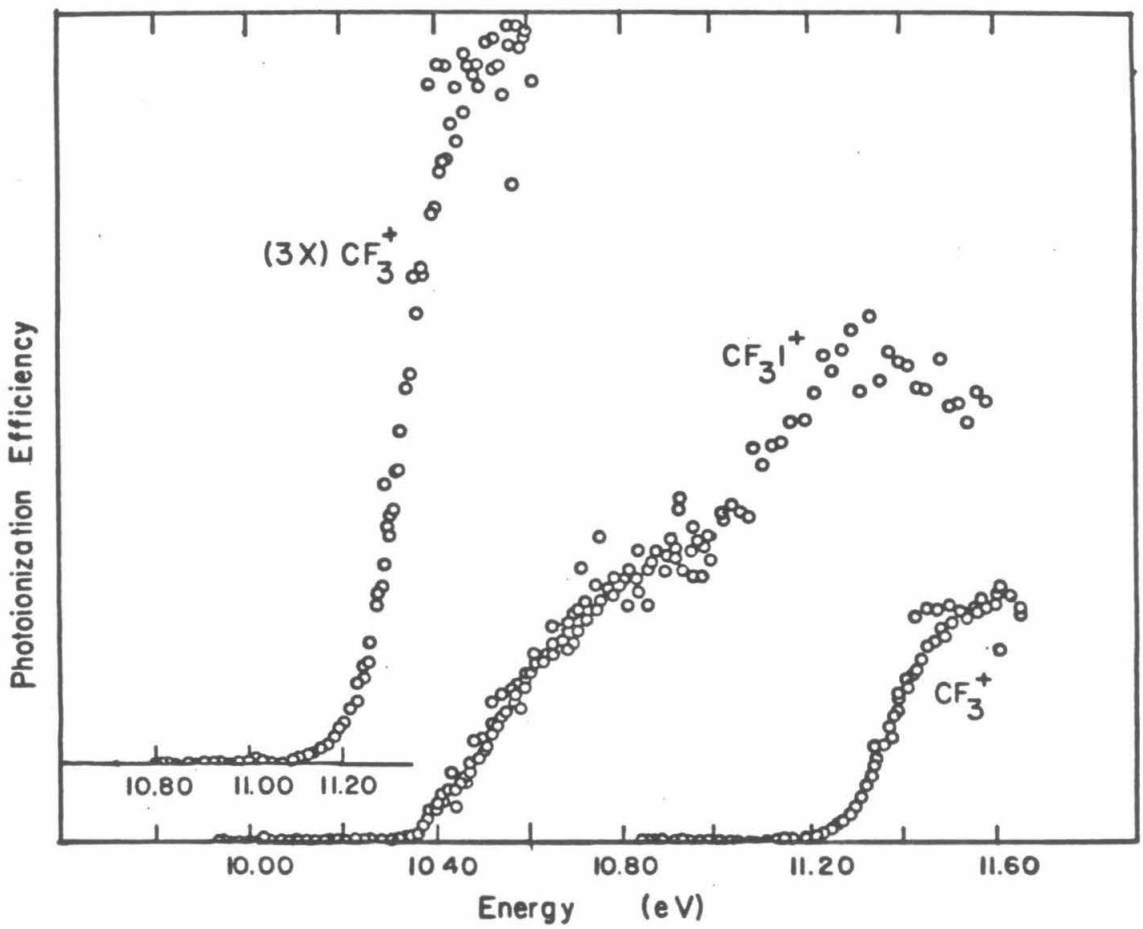
(3X) CF_3^+
CF_3I^+
CF_3^+
Photoionization Efficiency
10.80
11.00
11.20
10.00
10.40
10.80
11.20
11.60
Energy (eV)

$$CF_3I + h\nu \rightarrow CF_3^+ + I^- \qquad (5)$$

the earlier data. Such processes have been reported for other methyl halides [15], and would give a threshold lower by as much as 3.06 eV, the electron affinity of I [16]. To check for the presence of process (5), I^- was monitored as a function of photon energy. The results shown in Fig. 3 are observed using near zero repeller voltages. Two observations indicate that the source of I^- is not due to the pair process, Eq. (5). First, there is no correlation between the intensity of I^- and CF_3^+. Second, the I^- intensity is reduced significantly by increasing the repeller plate voltage, while CF_3^+ is not. Instead, I^- is produced from threshold photoelectrons in the two-step process described by Eqs. (6) and (7). Analogous processes have been observed in other systems and

$$CF_3I + h\nu_{th} \rightarrow CF_3I^+ + e^-(\sim 0\ \text{K.E.}) \qquad (6)$$

$$e^-(\sim 0\ \text{K.E.}) + CF_3I \rightarrow I^- + CF_3 \qquad (7)$$

are well characterized [17-20]. Figure 3 is therefore interpreted to be a threshold photoelectron spectrum by electron attachment (TPSA) [17-20]. The photoelectron spectrum of CF_3I has been studied in detail by Cvitaš et al. [14]. Their spectrum is included in Fig. 3 to show correspondence with the TPSA spectrum. Threshold energies determined for various processes in this and related work are presented in Table II, along with derived thermochemical information.

FIGURE 3. Comparison of the HeI photoelectron spectrum of CF_3I between 10 and 12 eV from ref. 14 and the threshold photoelectron spectrum by electron attachment (TPSA) of CF_3I.

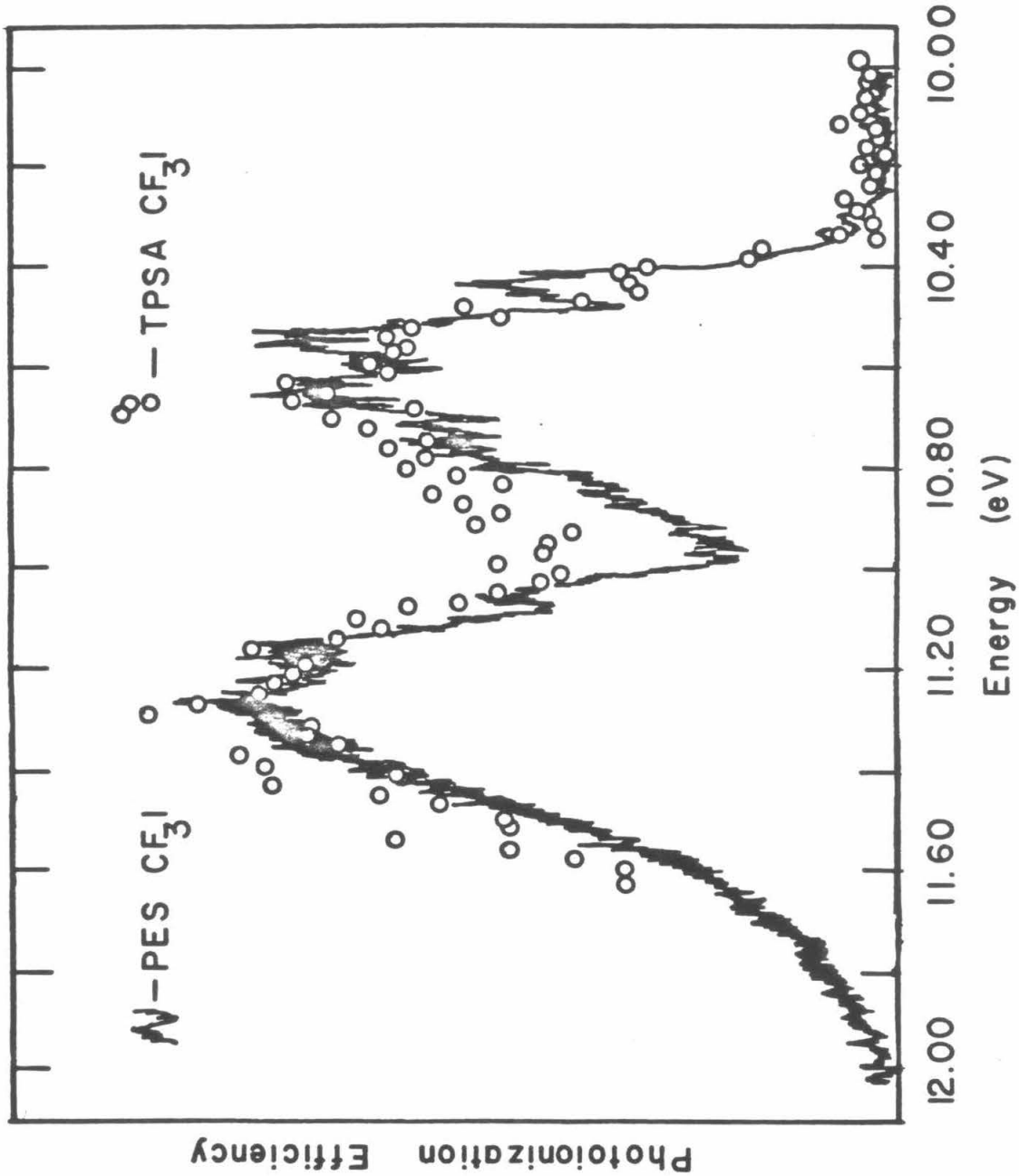
Photoionization Efficiency
12.00
11.60
11.20
10.80
10.40
10.00
Energy (eV)
PES CF_3I
TPSA CF_3I

DISCUSSION

Ion molecule reactions of CF_3I

The ion-molecule chemistry of CF_3I is simpler than previously suggested [1]. A comparison of the observed and calculated data in Fig. 1 illustrates the major features of this system are adequately described by a scheme employing reactions (2) to (4) alone. Here the calculated data are obtained from a least-squares fit of the four integrated rate equations to the observed data using the initial concentrations and rate constants as adjustable parameters. Statistical uncertainty in the calculated parameters is below 5% but uncertainty in the pressure measurements limits accuracy of the reported rate constants to ± 20%. Excellent agreement between the calculated and observed data further supports the conclusion that collision induced dissociation of CF_3I^+ does not occur. Thus the initial increase of CF_3^+ is due solely to reaction (2). Further, double resonance suggests that all three reactions are exothermic as supported by the thermochemical data in Table I. No endothermic or condensation processes were observed in the current experiments. However, the occurrence of condensation reactions in the previous work [1] is reasonable because of the high pressures used.

Thermochemistry

The value 10.32 ± 0.03 eV derived in this work for the adiabatic ionization potential of CF_3I compares, within experimental error, to the number measured by Cvitaš et al. [14]. The quantity 10.23 ± 0.02 eV given by Noutary [3] appears to be too low. $\Delta H^\circ_{f_0}$ (CF_3I^+) =

100.0 ± 1 kcal mole^{-1} is calculated from the 10.32 eV threshold (Table II).

From the 11.36 ± 0.03 eV 0° K adiabatic appearance potential for CF_3^+ derived in this work, $\Delta H_{f_0}^\circ$ (CF_3^+) = 98.3 ± 1 kcal mole^{-1} can be calculated. Within the uncertainty associated with such measurements, this is in excellent agreement with $\Delta H_{f_0}^\circ$ (CF_3^+) = 99.0 kcal mole^{-1} derived from a photoion-photoelectron coincidence study [2] of the appearance threshold for CF_3^+ from CF_4. The latter experiments have the potential to yield excellent thermochemical data, because they consider dissociation of a state selected molecular ion with well characterized internal energy and the kinetic energy of the product fragments is measured and accounted for. Comparing the various heats of formation of CF_3^+ summarized in Table III, values derived from the appearance threshold of CF_3^+ from C_2F_4 [4], and from direct ionization of CF_3 [4] also compare favorably with present results.

In general, discrepancies in the other values derived for the enthalpy of formation of CF_3^+ are due mainly to excess translational energy remaining in the product fragments [2-4]. However, thresholds published by Noutary [3] seem to be consistently low in the systems discussed. Considering the evidence as a whole, the best estimate for $\Delta H_{f_0}^\circ$ (CF_3^+) = 99.0 ± 1 kcal mole^{-1}, or $\Delta H_{f_{298}}^\circ$ (CF_3^+) = 98.3 kcal mole^{-1}.

TABLE II

Appearance thresholds and derived heats of formation

Neutral Precursor	Ion	IP[a]	AP[a]	$\Delta H_{f_0}^{\circ}$	$\Delta H_{f_{298}}^{\circ}$ [b]
CF_3I					
	CF_3I^+	10.23[c]			
		10.29[d]			
		10.32 ± 0.03[e]		100.0 ± 1[e]	98.6[e]
	CF_3^+		10.89[c]		
			11.36 ± 0.03[e]	98.3 ± 1[e]	97.6[e]

a Units are eV.

b Units are kcal $mole^{-1}$. Derived employing thermochemical information in Table III.

c Ref. 3.

d Ref. 14. See Results section of text.

e This work.

TABLE III

Relevant thermochemistry

Species	$\Delta H_{f_0}^{\circ}$ [a]	$\Delta H_{f_{298}}^{\circ}$ [a]	AP(CF_3^+) [b]	$\Delta H_{f_0}^{\circ}$ (CF_3^+) [c]	$\Delta H_{f_{298}}^{\circ}$ (CF_3^+) [c]
CF_4	-221.64	-223.04	15.52[d]	117.9	
			15.35[e]	114.0	
			14.7[f]	99.0	
CF_3Cl	-164.8	-166.0	12.81[g]	101.9	
			12.53[d]	95.5	
CF_3Br	-150.7	-153.6	11.83[h]	93.9	
			11.84[d]	94.2	
CF_3I	-138.0[i]	-139.4[i]	10.89[d]	87.5	
			11.36[j]	98.3	
C_2F_4	-156.6	-157.4	13.70[e]	99.2	
CF_3	-111.7	-112.4	9.17[e]	99.8	
			9.14[k]		
CF_3H	-162.84	-164.5			
F	18.38	18.88			
Cl	28.68	29.08			
Br	28.19	26.74			
I	25.63	25.54			
CF_3^+				99.0±1[l]	98.3±1[l]

a Units are kcal $mole^{-1}$. Values are taken from Ref. 16, except as noted.

TABLE III (continued)

b Units are eV. $AP(CF_3^+)$ are the 0° K adiabatic photoionization thresholds reported for production of CF_3^+ from the neutral species listed.

c Units are kcal $mole^{-1}$. Derived from $AP(CF_3^+)$.

d Ref. 3.

e Ref. 4.

f Ref. 2.

g Ref. 6.

h The values 11.71 eV from Ref. 3 was extrapolated to be 11.81 V at 0° K, Ref. 2.

i A careful investigation of the literature concerning determination of the neutral heats of formation cited, revealed that $\Delta H_f^\circ(CF_3Cl)$ and $\Delta H_f^\circ(CF_3Br)$ were measured relative to $\Delta H_f^\circ(CF_3I)$. (See: C. A. Goy, A. Lord and H. O. Pritchard, J. Phys. Chem., 71 (1967) 2705.) Further, $\Delta H_f^\circ(CF_3I)$ was measured relative to $\Delta H_f^\circ(CF_3H)$. (See: A. Lord, C. A. Goy and H. O. Pritchard, J. Phys. Chem., 71 (1967) 1086.) Thus, these values must remain correlated if precision is desired. This consistency was carefully maintained for values quoted in P. R. Stull and H. Prophet "JANAF Thermochemical Tables", 2nd ed. NSRDS-NBS 37 (U.S. Govt. Printing Office, Wash. D.C., 1971). When the numbers reported by Stull et al. were updated and transcribed in Ref. 16, their relative correlation was again maintained except for $\Delta H_f^\circ(CF_3I)$. Therefore, the number cited here for $\Delta H_f^\circ(CF_3I)$ is an extrapolation that is mutually consistent with the other

TABLE III (continued)

values discussed. ΔH_f° (CF_3I) = -138 kcal $mole^{-1}$ presented here is 1.6 kcal $mole^{-1}$ higher than in Ref. 16.

j This work.

k This number is calculated based on ΔH_{f_0} (CF_3^+) = 99.0 kcal $mole^{-1}$, Ref. 2.

l Best estimate from all of the data.

Acknowledgment

This work was supported by the California Institute of Technology Presidents fund. We also acknowledge Jocelyn C. Schultz for providing us with a photoelectron spectrum of CF_3I and A. S. Gaylord for writing the generalized least-squares computer program used to determine the rate constants.

REFERENCES

1 T. Hsieh, J. R. Eyler and R. J. Hanrahan, Int. J. Mass Spectrom. Ion Phys., 28 (1978) 113.

2 I. Powis, Mol. Phys., 39 (1980) 311.

3 C. J. Noutary, 1968 J. Res. Natl. Bur. Stand. A72, 479.

4 T. A. Walter, C. Lifshitz, W. A. Chupka and J. Berkowitz, J. Chem. Phys., 51 (1969) 3531.

5 L. Powis and C. Darby, J. Chem. Phys. Lett., 65 (1979) 390.

6 J. M. Ajello, W. T. Huntress and P. Rayerman, J. Chem. Phys. 64 (1976) 4746.

7 M. J. Coggiola and P. C. Cosby, J. Chem. Phys., 72 (1980) 6507.

8 L. R. Thorne and J. L. Beauchamp, J. Chem. Phys. submitted for publication.

9 J. L. Beauchamp, Annu. Rev. Phys. Chem., 22 (1971) 527.

10 J. L. Beauchamp, D. Holtz, S. D. Woodgate and S. L. Patt, J. Amer. Chem. Soc., 94 (1972) 279.

11 T. B. McMahan and J. L. Beauchamp, Rev. Sci. Instrum., 43 (1972) 509.

12 P. R. LeBreton, A. D. Williamson, J. L. Beauchamp and W. T. Huntress, J. Chem. Phys., 62 (1975) 1623.

13 A. D. Williamson, Ph.D. Thesis, California Institute of Technology, 1975.

14 T. Cvitaš, H. Güsten, L. Klasinc, I. Novak and H. Vančick, Z. Naturforsch. 32a (1977) 1528.

15 J. M. Ajello and P. Rayermann, J. Chem. Phys., 71 (1979) 1512.

REFERENCES (continued)

16 H. M. Rosenstock, K. Draxl, B. W. Steiner and J. T. Herron, J. of Phys. and Chem. Ref. Data, 6, Supplement No. 1.

17 J. M. Ajello and A. Chutjian, J. Chem. Phys., 65 (1976) 5524.

18 J. M. Ajello and A. Chutjian, J. Chem. Phys., 71 (1979) 1079.

19 A. Chutjian and J. M. Ajello, Chem. Phys. Lett., 72 (1980) 504.

20 J. M. Ajello, A. Chutjian and R. Winchell, J. Elect. Spect. and Rel. Phenom., 19 (1980) 197.